

# Effectiveness and Relationship between Biased and Unbiased Measures of Dopamine Release and Clearance

Anna C. Everett, Ben E. Graul, Joakim W. Ronström, J. Kayden Robinson, Daniel B. Watts, Rodrigo A. España, Cody A. Siciliano, and Jordan T. Yorgason\*



Cite This: *ACS Chem. Neurosci.* 2022, 13, 1534–1548



Read Online

ACCESS |



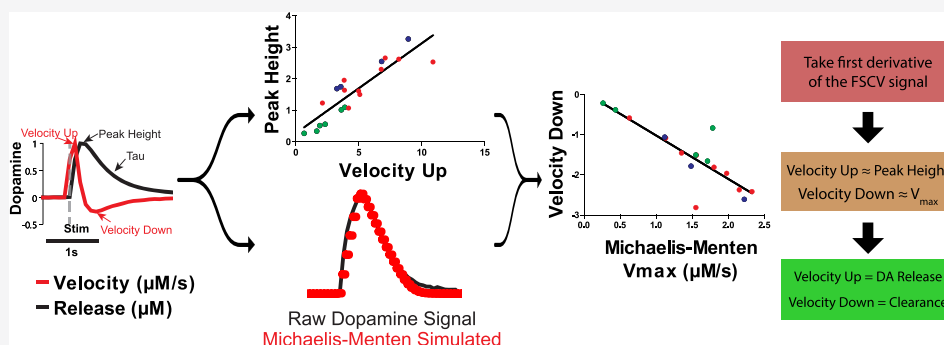
Metrics & More



Article Recommendations



Supporting Information



**ABSTRACT:** Fast-scan cyclic voltammetry (FSCV) is an effective tool for measuring dopamine release and clearance throughout the brain, especially the striatum where dopamine terminals are abundant and signals are heavily regulated by release machinery and the dopamine transporter (DAT). Peak height measurement is perhaps the most common method for measuring dopamine release, but it is influenced by changes in clearance. Michaelis–Menten-based modeling has been a standard in measuring dopamine clearance, but it is problematic in that it requires experimenter fitted modeling subject to experimenter bias. This study presents the use of the first derivative (velocity) of evoked dopamine signals as an alternative approach for measuring and distinguishing dopamine release from clearance. Maximal upward velocity predicts reductions in dopamine peak height due to  $D_2$  and  $GABA_B$  receptor stimulation and by alterations in calcium concentrations. The Michaelis–Menten maximal velocity ( $V_{max}$ ) measure, an approximation for DAT levels, predicts maximal downward velocity in slices and in vivo. Dopamine peak height and upward velocity were similar between wild-type and DAT knock-out (DATKO) mice. In contrast, downward velocity was lower and exponential decay ( $\tau$ ) was higher in DATKO mice, supporting the use of both measures for extreme changes in DAT activity. In slices, the competitive DAT inhibitors cocaine, PTT, and WF23 increased peak height and upward velocity differentially across increasing concentrations, with PTT and cocaine reducing these measures at high concentrations. Downward velocity and  $\tau$  values decreased and increased respectively across concentrations, with greater potency and efficacy observed with WF23 and PTT. In vivo recordings demonstrated similar effects of WF23, PTT, and cocaine on measures of release and clearance.  $\tau$  was a more sensitive measure at low concentrations, supporting its use as a surrogate for the Michaelis–Menten measure of apparent affinity ( $K_m$ ). Together, these results inform on the use of these various measures for dopamine release and clearance.

**KEYWORDS:** dopamine, dopamine transporter, fast-scan cyclic voltammetry, Michaelis–Menten, kinetics, striatum

## INTRODUCTION

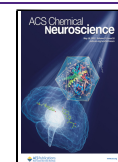
Fast-scan cyclic voltammetry (FSCV) is a widely used electrochemical detection technique that can be highly selective for specific analytes. This technique is perhaps most frequently used for the detection of monoamines (such as dopamine) and indolamines,<sup>1</sup> but is also increasingly used for detecting other neurotransmitters such as hydrogen peroxide and purines.<sup>2,3</sup> FSCV has good temporal resolution and chemical specificity, making it an ideal tool for studying the mechanisms underlying rapid neurotransmitter release and clearance. For the past 30 years, the Michaelis–Menten model has been used alongside voltammetry techniques to study the

kinetics of the dopamine transporter (DAT).<sup>4–7</sup> In general, the Michaelis–Menten equation is used to measure first order enzymatic kinetics, solute binding efficiency, and enzyme concentrations.<sup>8</sup> The maximal rate of dopamine uptake is a measure of DAT expression and identified as  $V_{max}$  and

**Received:** January 12, 2022

**Accepted:** April 15, 2022

**Published:** April 28, 2022



dopamine's apparent binding affinity for the DAT is the Michaelis–Menten constant ( $K_m$ ).

The voltammetry modified version of this model was described previously<sup>5–7</sup> and includes the typical  $V_{max}$  and  $K_m$  variables. The following modified Michaelis–Menten equation is commonly used to determine changes in release and DAT function.

$$\frac{d[DA]}{dt} = f[DA_p] - \frac{V_{max}}{\left(\left(\frac{K_m}{[DA]}\right) + 1\right)}$$

This equation models the change in evoked extracellular dopamine signal ( $[DA]$ ) from the presynaptic terminal across time, taking into account the frequency ( $f$ ) of the stimulating pulse, amount released per pulse (release rate constant,  $[DA_p]$ ), the maximal rate of dopamine uptake ( $V_{max}$ ), and the apparent binding affinity of dopamine for the DAT ( $K_m$ ). This equation makes several assumptions about the dopamine signal, such as a fixed amount of dopamine released per stimulation pulse, large enough signal that DAT transporters in the vicinity are saturated, and that the primary mechanism for clearing dopamine is through the DAT (as opposed to diffusion or another transporter). One additional variable included in this model is the thickness layer, which is a deconvolution factor used as a correction coefficient for improving model fit.<sup>5,6</sup>

The process for analyzing voltammetry data using these kinetic parameters is complicated and not completely standardized. Using the concentration vs time trace at the peak dopamine oxidation potential, data are imported into specialized software that allows for user-defined control over values from the model. The values are manually<sup>6,9–11</sup> or semi-automatically adjusted (e.g., using simplex fitting).<sup>7</sup> A second simulated curve is superimposed on the original, and correlation values are displayed so that the user can determine the fit of the curve. Having the curve fit by a computer algorithm reduces the experimenter bias, but can also be highly sensitive to noise.<sup>7</sup> Each of these methods allows for constraint of specific variables, which allows for hypothesis-driven modeling. One method for analysis is to have all the values adjusted (non-constrained) until a curve is fit.<sup>12</sup> Another common method is to start off with a specific fixed value for  $K_m$  (e.g., 160–200 nM based on previous dopamine binding studies<sup>13</sup>). With this fixed  $K_m$  value, only the thickness layer, release concentration, and  $V_{max}$  are adjusted to determine baseline release and clearance values.<sup>14–17</sup> This second method is often combined with a third approach where the  $V_{max}$  is constrained after drug application, and  $K_m$  becomes variable in the presence of psychostimulants.<sup>17–20</sup>

Although the use of these approaches has been effective at teasing out important physiological and pharmacological effects, choosing what values to constrain is at the discretion of the experimenter, resulting in an inherent experimenter bias. The overall strength of the fit can be determined by the Spearman's rank correlation coefficient.<sup>6</sup> However, the resulting  $V_{max}$  and  $K_m$  values can vary greatly depending on the constraints introduced by the experimenter performing the curve fitting. There are other methods that do not rely on experimenter-fitted models, such as computerized nonlinear regression.<sup>7</sup> However, these methods still rely on experimenter input on model constraints. As an alternative method, we showed previously that the exponential decay value tau

strongly relates to changes in apparent  $K_m$  (in the presence of psychostimulants).<sup>6</sup> In contrast,  $V_{max}$  did not correlate well with exponential decay measures.<sup>6</sup> Thus, the present work examines alternative methods for studying dopamine release and clearance kinetics involving the first derivative, or velocity, which is an easily replicable measure of slope across a time domain-based signal. Velocity values are compared across conditions known to influence dopamine release and clearance and compared to Michaelis–Menten model-based measures of  $V_{max}$  from slice and in vivo preparations. Unlike the Michaelis–Menten model, these analytical measures are not dependent on enzymatic activity, making them ideal for describing clearance in animal models that do not contain transporters. The present work describes this use of easily measurable values of slope that have reduced analytical bias and may inform on applications for studying dopamine clearance via the DAT, as well as diffusion and other non-DAT-mediated dopamine clearance.

## RESULTS AND DISCUSSION

**Upward Velocity and Peak Height as Measures of Changes in Dopamine Release.** In order to establish alternate measures of dopamine release, the maximal upward velocity was examined under conditions that alter release probability. The release curve and first derivative of an evoked dopamine signal (1 pulse) are shown (Figure 1A). Dopamine release was examined before and after the activation of two inhibitory G<sub>i</sub>-protein coupled receptors (GPCRs), GABA<sub>B</sub>, and D<sub>2</sub> receptors (Figure 1B,C). A maximal concentration of the GABA<sub>B</sub> agonist baclofen (30 μM) reduced NAc dopamine peak height by 30.1%, which reversed upon antagonist application (CGP55845; 200 nM). The D<sub>2</sub> agonist quinpirole (1 μM) reduced dopamine release to a much greater extent (92.7%), which similarly reversed with D<sub>2</sub> antagonist application (sulpiride; 600 nM). Peak height and velocity up strongly correlated in these experiments (Figure 1C;  $n = 35$  samples from 5 mice,  $r = 0.999$ , slope =  $5.006 \pm 0.008$ ,  $p < 0.001$ ). Michaelis–Menten  $V_{max}$  correlates to velocity up (Figure 1D;  $n = 35$  sample from 5 mice,  $r = 0.7$ , slope =  $1.99 \times x \pm 0.35$ ,  $p < 0.001$ ) and to velocity down (Figure 1E;  $n = 35$  sample from 5 mice,  $r = 0.84$ , slope =  $-0.89 \times x \pm 0.099$ ,  $p < 0.001$ ).

Electrically evoked dopamine release is calcium dependent,<sup>21,22</sup> and dopamine release at physiological calcium (~1.2 mM) levels is ~50% of release observed from maximal (2.4–4.8 mM) calcium concentrations.<sup>23</sup> Therefore, the effects of calcium (1.2–4.8 mM) on evoked dopamine release (20 Hz, 5p) were compared between peak height and upward velocity measures (Figure 2). Experiments with higher calcium (2.4–4.8 mM) concentrations exhibited ~232% greater dopamine release (200% for 2.4 mM, 263% for 4.8 mM) than physiological (1.2 mM) calcium levels (Figure 2A,B; one-way ANOVA,  $n_{1.2} = 6$  slices,  $n_{2.4} = 10$  slices,  $n_{4.8} = 4$  slices,  $F_{2,17} = 13.65$ ,  $p < 0.001$ ). Tukey's HSD posttest revealed significantly increased dopamine release differences between calcium concentrations (1.2–2.4 mM:  $p < 0.01$ ,  $q = 6.238$ ; 1.2 to 4.8 mM:  $p < 0.001$ ,  $q = 6.549$ ). Increasing calcium beyond standard FSCV concentration (from 2.4 to 4.8 mM) did not significantly increase dopamine release ( $p > 0.05$ ,  $q = 1.7$ ). Peak height correlated across increasing calcium concentrations for upward velocity (Figure 2C;  $n = 20$ ,  $r = 0.888$ , slope =  $0.286 \pm 0.0349$ ,  $p < 0.001$ ). This correlation was not as strong as that observed with baclofen and quinpirole experiments, possibly due to the use of multiple pulse

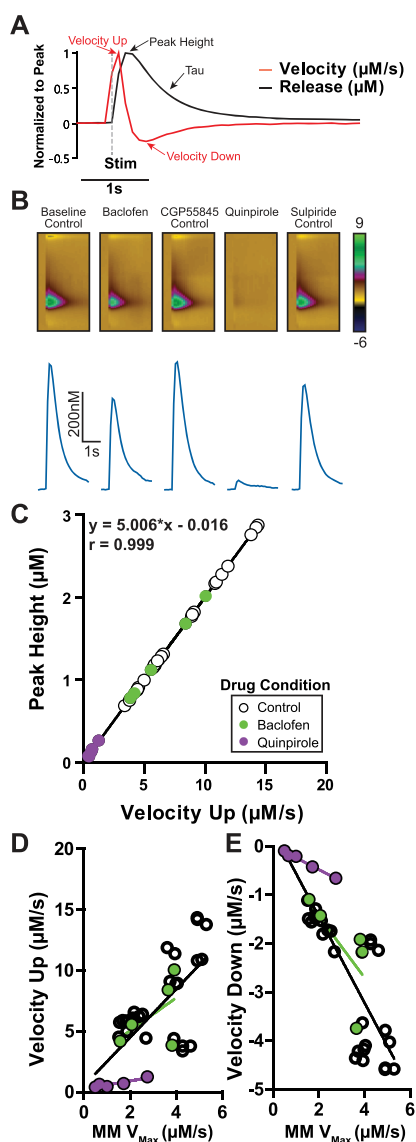


**Figure 1.** Peak height and upward velocity are related measures of dopamine release and are reduced with  $D_2$  and  $GABA_B$  agonists. (A) An example dopamine trace is shown under baseline conditions (black), alongside its corresponding first derivative (red; velocity), normalized by peak to highlight how these measures correspond to each other. Time of stimulation (1p, 30  $\mu$ A) is denoted (gray dashed line). (B) Dopamine release is reduced by  $GABA_B$  agonist baclofen (30  $\mu$ M), which is reversed by the  $GABA_B$  antagonist CGP55845 (200 nM), which acts as a control for baclofen effects. The  $D_2$  agonist quinpirole (1  $\mu$ M) robustly inhibits dopamine release, which is reversed by the  $D_2$  antagonist sulpiride (600 nM), which was also treated as a control condition. (C) Dopamine release peak height correlates with maximal upward velocity, which is decreased from control conditions during  $GABA_B$  and  $D_2$  stimulation. (D) Maximal upward and (E) maximal downward velocity significantly correlate to the Michaelis–Menten (MM)  $V_{max}$  values across all drug conditions.

stimulations, which may increase variability due to recruitment of additional feedback mechanisms. Thus, from GPCR-mediated inhibition experiments and calcium-dependent release experiments, there is a clear relationship between release peak height and the upward velocity of release. This is not surprising since velocity simply and effectively quantifies the rising slope of an existing curve. Changes in the relationship between upward velocity and peak would only

be expected if there were very large increases in peak height associated with decreased dopamine clearance, resulting in an overall decreased upward velocity. This idea is investigated later with psychostimulant application in slices.

Similar to the previous experiments, the Michaelis–Menten  $V_{max}$  correlates with velocity up (Figure 2D;  $n = 20$ ,  $r = 0.676$ , slope =  $0.145 \times x \pm 0.041$ ,  $p = 0.003$ ). More relevant to its value as a measure of dopamine uptake,  $V_{max}$  correlates strongly with velocity down (Figure 2E;  $n = 20$ ,  $r = 0.845$ , slope =  $-0.658 \times x \pm 0.108$ ,  $p < 0.001$ ). As evidence for velocity down working as a surrogate for  $V_{max}$ , voltammetry data were modeled using the described Michaelis–Menten approach, substituting velocity down for  $V_{max}$  and solving for DAp and  $K_m$  values. Signals where velocity down was substituted for  $V_{max}$  consistently correlated with fitted models ( $n = 16$ , mean Spearman  $r = 0.94 \pm 0.015$ ). This method of fixing  $V_{max}$  produced a mean  $K_m$  of  $200.2 \pm 11.93$  nM, which is in the range of  $K_m$  values used by others.<sup>7</sup> Three signals fit using this approach, and the resulting simulated curves, are demonstrated (Figure 2F) with examples from each calcium concentration. The subsequent experiments further explore downward velocity as a measure of dopamine clearance.

#### Downward Velocity as a Measure of DAT Function.

The predictive value of maximal downward velocity was investigated in relation to the Michaelis–Menten value  $V_{max}$ —an analytical value indicative of the maximal rate of dopamine clearance mediated by the DAT.<sup>4,6</sup> The Michaelis–Menten  $V_{max}$  measure was obtained under baseline (non-drug) conditions in brain slices (ex vivo; Figure 3A–C) and in anesthetized mice (in vivo; Figure 3D–F). The traces of evoked dopamine release (1 pulse) and first derivatives with low (blue) and high (green) downward velocity values from ex vivo recordings are shown (Figure 3A). Maximal downward velocity and Michaelis–Menten  $V_{max}$  values in brain slices are correlated (Figure 3B;  $n = 8$  slices,  $r = 0.79$ , slope =  $-0.158 \pm 0.05$ ,  $p = 0.02$ ). In vivo evoked (60 Hz, 30 pulses) dopamine release traces with low (orange) and high (pink) downward velocity rates are shown (Figure 3D). From in vivo experiments, downward velocity values correlated with Michaelis–Menten  $V_{max}$  values (Figure 3E;  $n = 9$  mice,  $r = 0.819$ , slope =  $-0.844 \pm 0.224$ ,  $p = 0.007$ ). Michaelis–Menten  $V_{max}$  values from these experiments in slice were much larger than in vivo values (ex vivo:  $2.463 \pm 0.472$ ; in vivo:  $1.025 \pm 0.094$   $\mu$ M/s; two-tailed  $t$ -test:  $t_{16} = 2.987$ ,  $p = 0.009$ ). In contrast, downward velocity values covered a similar range and were thus more comparable between in vivo and ex vivo conditions, though there were significant differences between downward velocity values under the two conditions (ex vivo:  $-1.059 \pm 0.095$ ; in vivo:  $-0.698 \pm 0.084$   $\mu$ M/s; two-tailed  $t$ -test:  $t_{14} = -2.472$ ,  $p = 0.027$ ). The source of this variability between preparations is unknown, but may reflect inherent differences in recording conditions (e.g., stimulation settings, extracellular conditions) making it difficult to compare across preparations. Importantly, the relationship between upward velocity and  $V_{max}$  that exists under  $G_i$  stimulation and varying calcium conditions does not exist in normal baseline conditions (Supporting Information Figure 1A, ex vivo:  $n = 8$  slices,  $r = 0.208$ , slope =  $0.364 \pm 0.698$ ,  $p = 0.621$ ; Supporting Information 1C, in vivo:  $n = 8$  slices,  $r = 0.528$ , slope =  $1.058 \pm 0.643$ ,  $p = 0.144$ ). This suggests that upward velocity is a better predictor when there are large changes in  $V_{max}$  as opposed to the small differences in  $V_{max}$  that may exist between subjects.

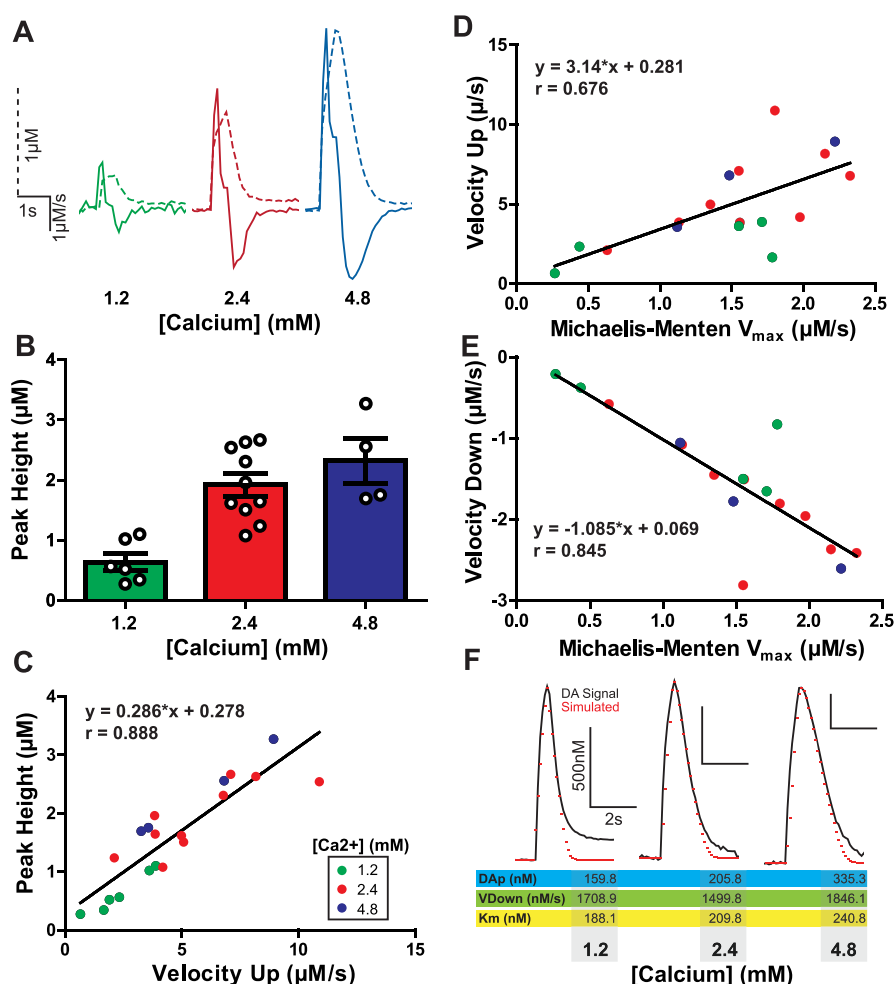


**Figure 2.** Upward velocity and peak height as measures of changes in dopamine release with calcium. (A) A comparison of example dopamine traces (dotted lines) overlaid with the corresponding first derivative (solid lines) at increasing concentrations of calcium. All traces are scaled identically. (B) Maximal evoked dopamine concentrations ( $\mu\text{M}$ ) at increasing concentrations of calcium (mM). (C) Maximal upward velocity corresponds linearly with an increase in evoked dopamine release. Calcium concentrations for each measure are denoted by color. (D) Upward velocity and (E) downward velocity correlate with the Michaelis–Menten  $V_{\text{max}}$  across all calcium conditions. (F) Voltammetry signals were modeled using Michaelis–Menten protocols where the maximal downward velocity was substituted for the  $V_{\text{max}}$  value. Shown are three example traces (black) from each calcium condition overlaid with simulated modeled data (red) from these experiments. Below the traces are the Michaelis–Menten parameters obtained through modeling with downward velocity as the  $V_{\text{max}}$ .

The exponential decay constant  $\tau$  is a simple and commonly used method for describing dopamine uptake kinetics.<sup>6</sup> Thus,  $\tau$  was compared to Michaelis–Menten  $V_{\text{max}}$  (Figure 3C,F) and downward velocity (Supporting Information Figure 1B,D) values *ex vivo* and *in vivo*.  $\tau$  was not significantly correlated with  $V_{\text{max}}$  ( $n = 9$  mice,  $r = 0.372$ , slope =  $-2.227 \pm 2.098$ ,  $p = 0.324$ ) or maximal velocity down ( $n = 8$  slices,  $r = 0.516$ , slope =  $-0.139 \pm 0.094$ ,  $p = 0.19$ ). Thus, while previous studies show that  $\tau$  is effective for measuring general changes in dopamine uptake and correlates with the Michaelis–Menten  $K_m$ , it is not a suitable replacement for  $V_{\text{max}}$ . This is consistent with our previous comparison.<sup>6</sup> These data support the idea that  $\tau$  and downward velocity measure fundamentally different processes, and suggest that both measures of uptake are useful for determining changes to the multifaceted process. For the remaining experiments, peak, upward velocity, downward velocity, and  $\tau$  will be explored in the context of genetic and pharmacological DAT inactivation.

#### Downward Velocity as a Measure of Dopamine Clearance in DAT Knockout Mice. Peak height and

downward velocity measures were examined in DATKO mice to determine how much the DAT contributes to these measures (Figure 4). Since downward velocity is an effective predictor at measuring DAT function in relation to the Michaelis–Menten  $V_{\text{max}}$  measure, it was expected that this measure would be most affected by DAT removal. Furthermore, Michaelis–Menten parameters cannot be tested in DATKO mice due to violation of modeling parameters from complete lack of DAT enzymatic activity.<sup>5</sup> Dopamine signals were examined at three stimulation conditions that produce varying dopamine release concentrations (1 pulse, 5 pulses at 20 Hz, 24 pulses at 60 Hz). Example dopamine release (Figure 4A) and velocity (Figure 4B) traces are shown. Upward velocity positively correlated with peak height in WT mice (velocity:  $n = 46$ ,  $r = 0.838$ ,  $p < 0.001$ , slope =  $1.92 \pm 0.19$ ) and in DATKO mice (velocity:  $n = 36$ ,  $r = 0.801$ ,  $p < 0.001$ , slope =  $1.59 \pm 0.2$ ). The relationship between peak dopamine and upward velocity (across stimulation conditions) was examined, and no significant difference was observed between WT and DATKO mice ( $F_{1,78} = 1.38$ ,  $p = 0.243$ ). Therefore, peak dopamine signals from multiple pulse stimulations relate



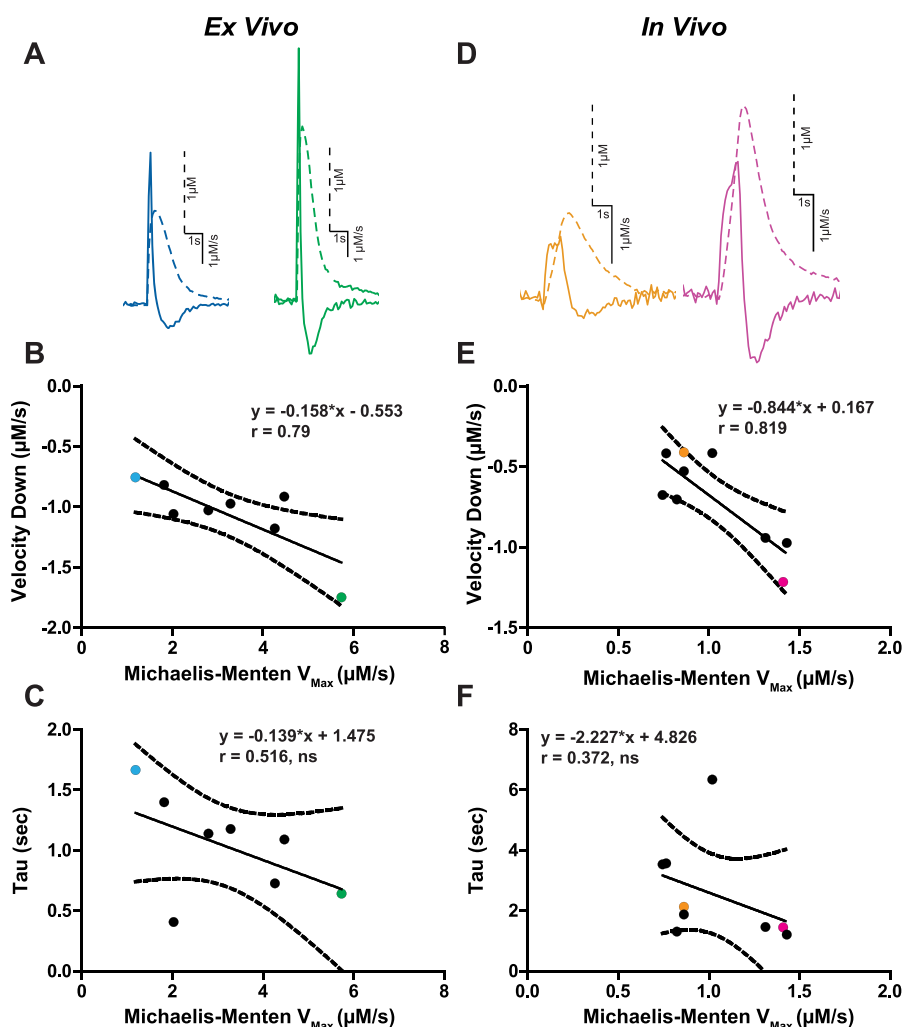


**Figure 3.** Downward velocity as a measure of dopamine transporter function. Evoked dopamine traces from ex vivo (A) and in vivo (D) recordings. Traces are scaled individually. Dopamine concentration (dotted lines) and first derivative (solid line) are overlaid. Each trace is scaled individually. (B) The  $V_{\max}$  obtained using the Michaelis–Menten model is plotted against the descending arm of the first derivative (Velocity Down). Each dot represents one experiment from ex vivo (B) and in vivo (E) experiments, with the colored dots corresponding to their respective colored traces in panels A and D. The exponential decay measure tau was examined against  $V_{\max}$ , and the two measures did not significantly correlate for ex vivo (C) and in vivo (F) experiments. (ns, not significant).

to maximal upward velocity measures, and this relationship was maintained in the absence of the DAT. Two-way repeated measures ANOVA for peak release (Figure 4C) revealed a main effect of stimulation intensity ( $F_{2,56} = 186.74$ ,  $p < 0.001$ ), but no effect of mouse strain ( $F_{1,56} = 2.65$ ,  $p = 0.115$ ) and no significant interaction ( $F_{2,56} = 1.25$ ,  $p = 0.294$ ). For upward velocity (Figure 4D,E) there was a main effect of stimulation intensity ( $F_{2,56} = 68.48$ ,  $p < 0.001$ ), but no effect of mouse strain ( $F_{1,56} = 0.70$ ,  $p = 0.408$ ) and no significant interaction between these terms ( $F_{2,56} = 0.27$ ,  $p = 0.766$ ). Thus, detection of release as measured by peak and upward velocity is increased with higher stimulation intensities and is similar between WT and DATKO mice.

Dopamine clearance was evaluated using striatal slices from WT and DATKO mice (Figure 5). Average ( $\pm$  SEM) first derivative curves across an evoked release time course are shown (Figure 5A; 20 Hz, 5 pulse stimulation). There are clear differences in overlap for the downward velocity slope in these two strains. A subtraction between average dopamine velocity curves from WT and DATKO mice across stimulation conditions highlights the time course of velocity differences

(Figure 5B). Interestingly, greater downward velocities were observed with higher stimulation intensity (compare green 5 pulse curve to black 1 pulse curve in Figure 5B), with greatest velocities observed in WT mice at the 60 Hz 24 pulse stimulation conditions (WT 1p:  $-1.395 \mu\text{M/s}$ ; WT 20 Hz 5p:  $-1.963 \mu\text{M/s}$ ; WT 60 Hz 24p:  $-2.138 \mu\text{M/s}$ ). Not surprisingly, longer duration stimulations also resulted in subtraction curves with longer duration downward velocities. These results show that DAT effects across time can be more pronounced with longer stimulations. Maximal downward velocity values across stimulation conditions and strains are shown (Figure 5C). Two-way repeated measures ANOVA for downward velocity revealed a main effect of stimulation intensity ( $F_{2,56} = 23.27$ ,  $p < 0.001$ ) and mouse strain ( $F_{1,56} = 12.33$ ,  $p = 0.002$ ), but no significant interaction between these terms ( $F_{2,56} = 1.58$ ,  $p = 0.215$ ). Two-way repeated measures ANOVA for tau (Figure 5D) revealed a main effect of mouse strain ( $F_{1,56} = 58.13$ ,  $p < 0.001$ ), but no significant main effect of stimulation intensity ( $F_{2,56} = 1.93$ ,  $p = 0.155$ ) nor a significant interaction between these terms ( $F_{2,56} = 1.00$ ,  $p = 0.376$ ). These DATKO experiments highlight the utility of

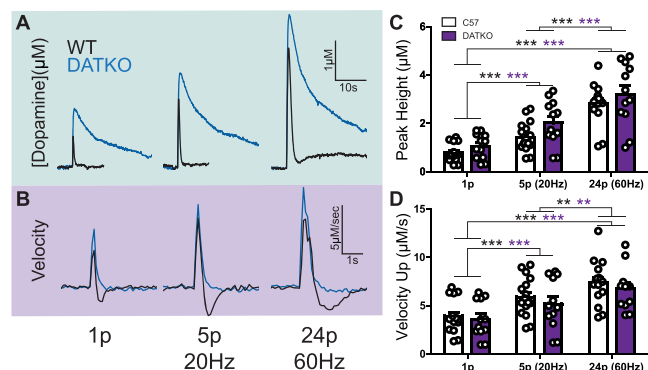


**Figure 4.** Upward velocity is not indicative of difference in uptake in DAT knockout mice. (A) Evoked dopamine release concentrations compared between wild-type (black) and DAT knockout (blue) mice. Increasing pulse number and frequency induced higher release concentrations. Pulse protocols began with a single pulse (left), then increased to 5 pulses at 20 Hz (middle) and ended with 24 pulses at 60 Hz (right). (B) The first derivative (velocity) of the dopamine traces in panel A. (C) Average peak dopamine concentrations for the three pulse conditions. Each dot represents a single pulse event. (D) First derivative maximum (peak velocity) for the three pulse conditions. Each dot represents a single pulse event. (\*\* =  $p < 0.01$ ; \*\*\* =  $p < 0.001$ ).

downward velocity for measuring large changes in dopamine uptake by complete removal of the DAT. While tau can measure drastic differences between mouse strains, it is not as sensitive as downward velocity for measuring changes in rapid uptake related to stimulation intensity.

**DAT Blockers Differential Effects on Release and Uptake.** DAT inhibitors of the tropane family share a DAT binding site with dopamine.<sup>24–26</sup> Therefore, it is expected that due to competition effects, downward velocity will have varying sensitivity to DAT inhibitors that will be weakest at lowest concentrations and strongest with inhibitors with higher affinity. The effects of tropane DAT competitive blockers with varying affinities (WF23, PTT, cocaine) on dopamine clearance was measured ex vivo (Figure 6). Representative release traces are shown for WF23 (Figure 6A), PTT (Figure 6B), and cocaine (Figure 6C). The highly potent WF23 ( $K_i = 0.1$  nM)<sup>27</sup> elevated peak height (Figure 6D) across increasing concentrations (10 nM–3 μM), with the greatest increases observed at the 300 nM concentration at ~458% of baseline. Similarly, PTT ( $K_i = 3$ –8.2 nM; 100 nM–30 μM)<sup>28,29</sup> increased peak height with greatest effects at 1 μM (~282% of baseline). Cocaine ( $K_i = 120$ –189 nM; 300 nM–30 μM)<sup>30,31</sup> elevated peak height to a maximum of ~134% baseline at 1–3 μM. Uniquely, cocaine also decreased signals by ~49% from baseline at 30 μM. Although WF23 and PTT both exhibited an inverted U-shaped curve, peak height never fell below baseline levels for these drugs. Two-way ANOVA on peak height data revealed a main effect of concentration ( $F_{8,60} = 6.28$ ,  $p < 0.001$ ), but indicated no drug effect ( $F_{2,60} = 0.06$ ,  $p = 0.942$  or interaction ( $F_{1,60} = 1.51$ ,  $p = 0.126$ ).

The upward velocity measures were affected differently than peak height by competitive DAT inhibitors. The greatest effects for upward velocity across the three drugs were at 100 nM for WF23 (~194%) and 300 nM concentrations for PTT (~112%) and cocaine (~118%; Figure 6E). Upward velocity reduced below baseline at >1 μM (WF23, PTT) and >10 μM (cocaine) concentrations. This is an important example where increases in peak height do not relate directly to upward

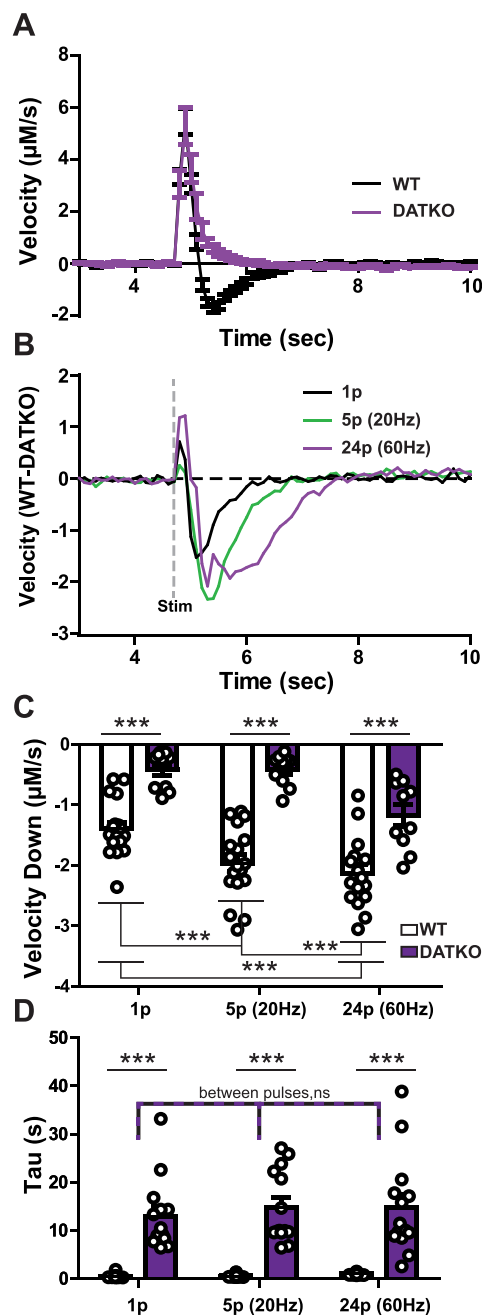


**Figure 5.** Downward velocity as a measure of dopamine clearance in DAT knockout mice. (A) A comparison of wild-type (black line) and DAT knockout (purple line) velocities obtained via the first derivative of dopamine concentration release under the single pulse condition. Note the slow decrease in DATKO compared to the negative values in the WT mouse. (B) A subtraction plot of a first derivative trace in a WT mouse minus a trace from the DATKO mouse for each pulse condition. An electrical stimulation was delivered at 5 s as denoted by the dashed gray line. (C) Average minima for the first derivative (peak velocity down) and (D) exponential decay measure tau compared by mouse type and pulse condition. Each dot denotes a single dopamine release event. (\*\*\*) =  $p < 0.001$ ; ns, not significant).

velocity and suggests that the increase in peak height observed at the higher concentrations of inhibitors is likely due to a different mechanism, such as increased spread from distant dopamine terminals. This phenomenon can be observed in traces from WF23 and PTT experiments at high concentrations, where the peak height is larger than the baseline, and

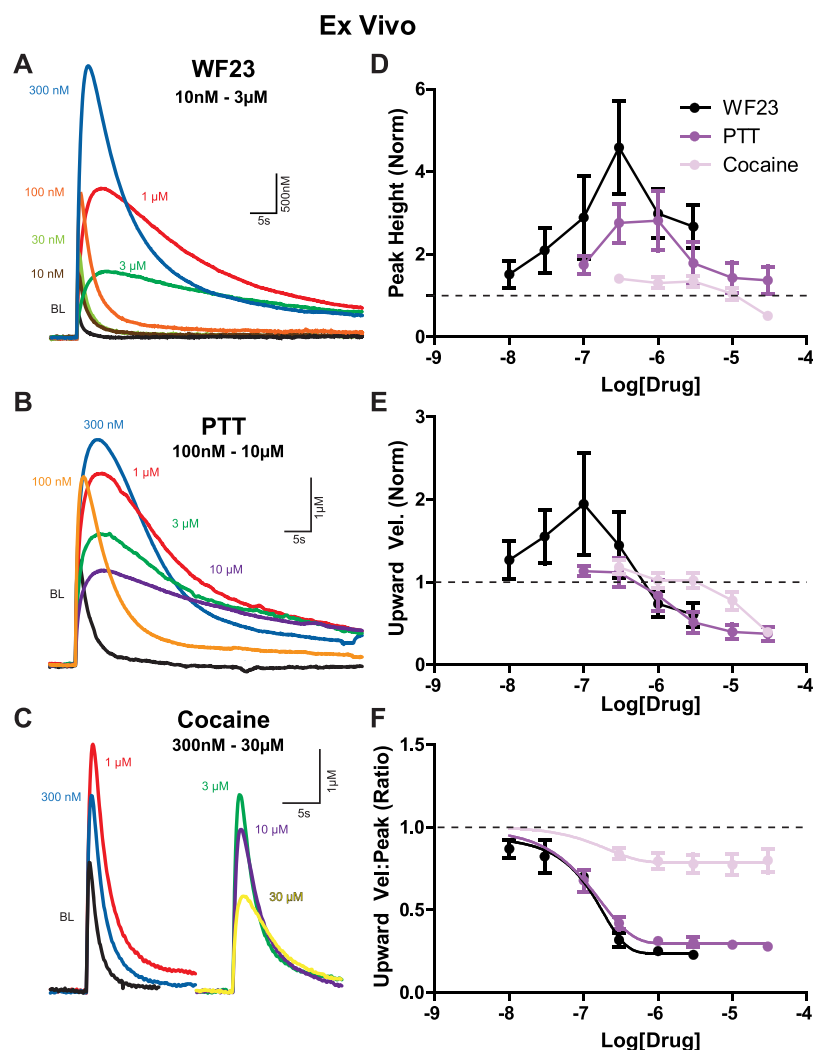


**Figure 6.** Effects of DAT blockers on dopamine release kinetics ex vivo. Traces from (A) WF23 (10 nM–3  $\mu$ M), (B) PTT (100 nM–30  $\mu$ M), and (C) cocaine (300 nM–30  $\mu$ M) drug concentrations found in Figure 6D–F, respectively. Signals denoted by color: baseline (black), 10 nM (brown), 30 nM (yellow-green), 100 nM (orange), 300 nM (blue), 1  $\mu$ M (red), 3  $\mu$ M (green), 10  $\mu$ M (dark purple), 30  $\mu$ M (yellow). (D) Comparison of peak height of signals across concentrations for WF23 (black), PTT (purple), and cocaine (pink). Similar comparisons across drug concentrations for (E) upward velocity and (F) the ratio of upward velocity to peak height. All measurements are normalized to baseline.

the time to peak is delayed (rightward shifted), reflecting a slower upward velocity (Figure 6A,B). Two-way ANOVA on upward velocity data revealed a main effect of concentration ( $F_{8,60} = 4.19$ ,  $p < 0.001$ ), no drug effect ( $F_{2,60} = 0.73$ ,  $p = 0.45$ ), and no interaction ( $F_{1,60} = 1.20$ ,  $p = 0.291$ ).

Since the association between upward velocity and peak height is weaker in the presence of high concentrations of DAT blockers, this measure may be particularly useful in dissociating and interpreting mechanisms underlying increases in peak height that are not due to increased vesicular fusion. The ratio between upward velocity and peak height was examined across drug concentrations (Figure 6F) and exhibited a clear decrease for all DAT blockers, with greater efficacy and potency for WF23 and PTT over cocaine. Two-way ANOVA on the ratio between upward velocity and peak height data revealed a main effect of concentration ( $F_{8,60} = 70.35$ ,  $p < 0.001$ ), a main effect of drug ( $F_{2,60} = 12.16$ ,  $p = 0.001$ ), and a significant interaction ( $F_{1,60} = 8.45$ ,  $p < 0.001$ ).

The effects of tropane analogs on downward velocity in striatal slices was examined next (Figure 7). First derivative traces are shown for WF23, PTT, and cocaine (Figure 7A–C).

All three drugs reduced downward velocity at high concentrations (Figure 7D), but effects were mixed at low (<100 nM) concentrations, with WF23 in some experiments exhibiting faster (more negative) downward velocity (see example traces in Figure 7A). Therefore, WF23 effects were examined with (Figure 7D) and without (inset) experiments where velocity increased at low concentration ranges. For WF23 and PTT experiments, downward velocity was reduced for a similar range of concentrations (>100 nM), which was leftward shifted from cocaine, reflective of the increased potency of WF23 and PTT for the DAT over cocaine. Cocaine effects were modest (apparent effects at  $\geq 30$   $\mu$ M) and did not plateau until  $\geq 30$   $\mu$ M. These data suggest that downward velocity is an effective tool for measuring relative potency for competitive DAT inhibitors.

The Michaelis–Menten  $K_m$  is frequently used for describing the effects of DAT inhibitors<sup>19,20,32,33</sup> and correlates strongly with the exponential decay measure  $\tau$ .<sup>6</sup> Therefore, in order to establish the relationship between exponential decay and downward velocity, the effects of tropane analogs on  $\tau$  were examined (Figure 7E).  $\tau$  was more sensitive to tropane

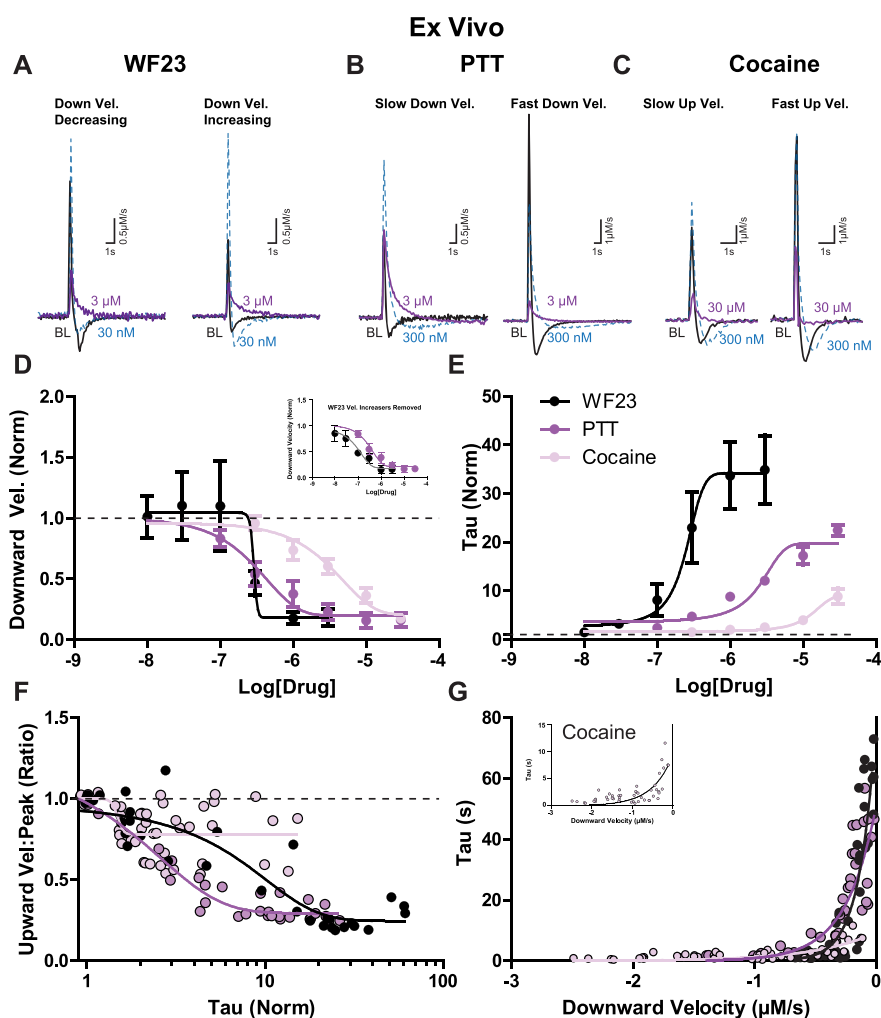


**Figure 7.** Effects of DAT blockers on dopamine uptake kinetics ex vivo. Example first derivative traces are shown under baseline conditions (black), 30 nM (blue), and 3 μM (purple) for (A) WF23, (B) PTT, and (C) cocaine. (A) three experiments indicated a distinct decrease in downward velocity with addition of WF23 at a low concentration (left) while in two experiments the downward velocity increased (right). (B) experiments with slower downward velocity at baseline (left) are shown next to signals with faster downward velocity at baseline (right). (C) experiments with slower upward velocity at baseline (left) are depicted next to signals with fast upward velocity at baseline (right). (D) Downward velocity (normalized) and (E) tau (normalized) are compared across increasing concentrations of WF23 (black), PTT (purple), and cocaine (pink). (F) Relationship between tau (normalized) and the ratio of upward velocity to peak height for each drug. (G) Relationship between downward velocity (μM/s) and tau (s) for each drug.

analogs than downward velocity, with WF23 increasing tau with the greatest efficacy and potency ( $\text{LogEC}_{50} = 0.242$ ), followed by PTT ( $\text{LogEC}_{50} = 2.326$ ) and cocaine ( $\text{LogEC}_{50} = 12.59$ ). Two-way ANOVA on tau data revealed a main effect of concentration ( $F_{8,60} = 13.90$ ,  $p < 0.001$ ) and a significant interaction between these terms ( $F_{16,60} = 4.69$ ,  $p < 0.001$ ), but no main effect of drug ( $F_{2,60} = 2.51$ ,  $p = 0.12$ ). Considering the increased sensitivity of tau over downward velocity in measures of psychostimulant sensitivity, downward velocity appears more effective at measuring changes in dopamine uptake reflective of changes in transporter numbers (similar to  $V_{\text{max}}$ ), while tau appears more effective for detecting changes in apparent affinity of dopamine for the DAT (similar to  $K_{\text{m}}$ ).

Decreases in the upward velocity to peak height ratio (seen in Figure 6F) may be due to reduced dopamine clearance. Since tau is a sensitive measure of impaired clearance for competitive inhibition (Figure 7E), the relationship between these two values was examined. Upward velocity to peak ratio correlated to tau (Figure 7F) for WF23 (Spearman  $r = -0.82$ ,

$p < 0.001$ ) and PTT (Spearman  $r = -0.862$ ,  $p < 0.001$ ) and significantly, but less for cocaine (Spearman  $r = -0.3802$ ,  $p = 0.0077$ ), likely reflecting cocaine's lower efficacy at reducing the upward velocity to peak height ratio and lower efficacy on increasing tau. These data highlight the relationship between increases in dopamine signals and decreases in uptake which are most apparent as tau increases but are different for each competitive inhibitor. The relationship between tau and downward velocity was further examined in the context of DAT inhibitors (Figure 7G). Tau values significantly correlated with downward velocity for WF23 (Spearman  $r = 0.784$ ,  $p < 0.001$ ) PTT (Spearman  $r = 0.894$ ,  $p < 0.001$ ) and cocaine (Spearman  $r = 0.652$ ,  $p < 0.001$ ), and tau was most strongly related at smaller downward velocities. Therefore, reductions in upward velocity to peak ratio are due in part to impaired clearance, and tau becomes more predictive of downward velocity in conditions where dopamine clearance is severely impaired by reuptake inhibitors.



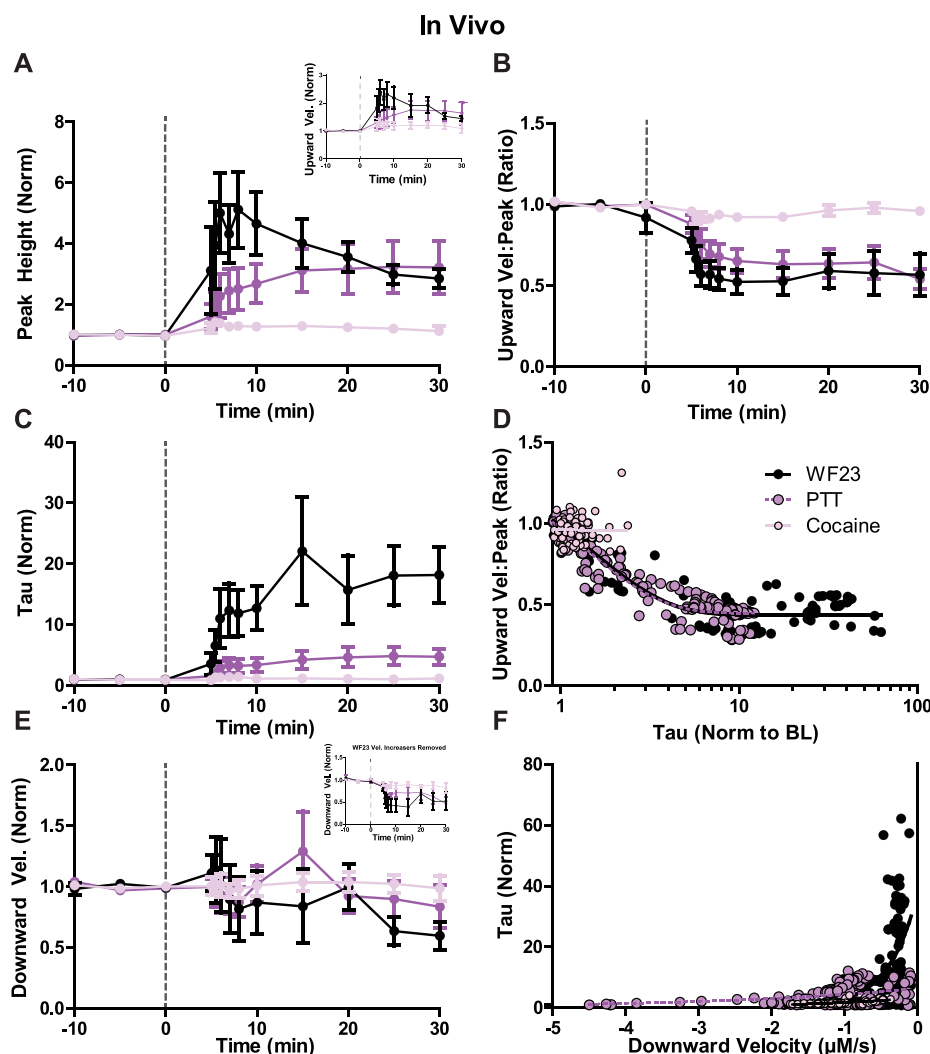


**Figure 8.** Effects of DAT blockers on dopamine release and uptake kinetics in vivo. Time course of psychostimulants on dopamine transmission across 30 min (post-injection) as measured by (A) peak height, upward velocity (inset), (B) ratio of upward velocity to peak height, (C) exponential decay (tau), and (E) downward velocity for WF23 (black), PTT (purple), and cocaine (pink). All values normalized to baseline. (D) Comparison of tau (normalized) to ratio of upward velocity to peak height for each drug across the full time course. (F) Comparison of downward velocity ( $\mu\text{M/s}$ ) to tau (normalized) for each drug.

The effects of potent competitive DAT inhibitors (WF23 and PTT) and a less potent inhibitor (cocaine) were tested in vivo in order to establish a measure of sensitivity for these three different drugs. Experiments were performed across a 30-min time course, and measures of peak height, upward velocity, downward velocity, and tau were all examined (Figure 8). To compare the effect of each drug, one-way ANOVAs were conducted at the peak effect of each measure. Peak height was significantly different between WF23, PTT, and cocaine with a much larger increase in WF23 and PTT in comparison to cocaine (Figure 8A: One-way ANOVA;  $F_{2,17} = 4.49$ ,  $p = 0.027$ ). Upward velocity was trending toward significance with slightly higher velocity values using WF23 and PTT (Figure 8A Inset: One-way ANOVA;  $F_{2,17} = 3.011$ ,  $p = 0.076$ ). However, when we compared the ratio of upward velocity to peak height, there was a strong significant difference across the three drugs (Figure 8B: One-way ANOVA;  $F_{2,17} = 11.338$ ,  $p = 0.0007$ ). Tau was much higher in WF23 in comparison to PTT, and tau was higher in PTT than cocaine (Figure 8C: One-way ANOVA;  $F_{2,16} = 8.763$ ,  $p = 0.0027$ ). The upward velocity to peak ratio correlated with changes in tau (Figure 8D) for

WF23 (Spearman  $r = -0.606$ ,  $p < 0.001$ ) and PTT (Spearman  $r = -0.938$ ,  $p < 0.001$ ), but did not correlate with cocaine (Spearman  $r = -0.099$ ,  $p = 0.333$ ). However, there was no significant difference in downward velocity between drugs, and quite a lot of variability (Figure 8E: one-way ANOVA;  $F_{2,17} = 1.892$ ,  $p = 0.181$ ). Interestingly, in some WF23, PTT, and cocaine experiments the downward velocity increased initially (Figure 8E; during the first 20 min; two-way RM-ANOVA; time effect:  $F_{12,68} = 1.57$ ,  $p = 0.12$ ; drug effect:  $F_{1,68} = 0.41$ ,  $p = 0.544$ ; interaction:  $F_{12,68} = 0.49$ ,  $p = 0.091$ ), likely due to initial low concentration effects on increasing DAT activity, which were also observed in slices (Figure 7A,D). When these increasing values are removed, there is a clear decrease in downward velocity induced by WF23, PTT, and cocaine at the 5 second time points, with effects ordered by drug potency (Figure 8E Inset; two-way RM-ANOVA; time effect:  $F_{12,20} = 3.4$ ,  $p = 0.008$ ; drug effect:  $F_{1,20} = 1.24$ ,  $p = 0.381$ ; interaction:  $F_{12,20} = 0.45$ ,  $p = 0.92$ ). Similar to slice experiments, downward velocity from in vivo experiments correlated with tau (Figure 8F) for WF23 (Spearman  $r = 0.688$ ,  $p < 0.001$ ), PTT

(Spearman  $r = 0.244$ ,  $p = 0.007$ ), and cocaine (Spearman  $r = 0.659$ ,  $p < 0.001$ ).

The present experiments examine measures of dopamine release and clearance. Dopamine peak height is reduced by application of GABA<sub>B</sub> and D<sub>2</sub> agonists and increased with enhanced calcium levels and greater stimulation intensity. This release measure correlated strongly with maximal upward velocity. Maximal downward velocity correlated with the Michaelis–Menten uptake measure of  $V_{\max}$ , an indirect measure of DAT expression, whereas the exponential decay measure tau related more to the Michaelis–Menten measure  $K_m$ . Genetic and pharmacological blockade of the DAT resulted in concentration-dependent reductions in the observed maximal downward velocity and increases in tau, with greatest sensitivity in the latter measure. The application of these measures to dopamine signals introduces an unbiased approach for measuring release and clearance, which is needed for improving analysis standardization across the field.

The relationship between drug-induced changes in peak height and upward velocity is complex and represents a concert between cellular mechanisms underlying release and clearance. In conditions where release is solely influenced, increases in peak height are tightly related to velocity increases. In contrast, for tropane concentration response experiments, peak height increased across drug concentrations, but the velocity of the rising peak varied greatly in a drug and concentration-dependent manner (increasing at low and decreasing at high concentrations respectively). Peak height increases associated with slower upward velocities indicate the crude nature of peak height as a measure of release alone. The dissociation between these measures apparent in the presence of DAT blockers is indicative of the multitude of effects of these drugs on dopamine terminal function.

The modified voltammetry Michaelis–Menten model is used to calculate the amount of dopamine released ( $[DA_p]$ ) in the context of DAT enzymatic activity values ( $V_{\max}$  and  $K_m$ ).<sup>5</sup> This same model was previously used to measure cocaine's DAT-blocking effects and comparisons were made across dopamine signal peak height,  $[DA_p]$ ,  $K_m$  and the area under the curve.<sup>6</sup> From these previous experiments, peak height correlated strongly with  $[DA_p]$  ( $r = 0.97$ ) across cocaine concentrations (300 nM–30  $\mu$ M). Presently, similar increases in peak height were observed across concentrations of DAT blockers, with increases above baseline for most concentrations, and slight reductions in dopamine peak with cocaine at 30  $\mu$ M (reduced by ~20%). As a comparison, upward velocity increased at concentrations  $\leq 1$   $\mu$ M for WF23/PTT (peak increases of ~32–57% at 300 nM, respectively) and  $\leq 3$   $\mu$ M for cocaine (peak increases of ~33% at 300 nM). In contrast, upward velocity decreased at higher concentrations (~18% decreases with WF23 at 3  $\mu$ M; ~33–42% decreases with PTT at 10–30  $\mu$ M; ~13–48% decreases with cocaine at 10–30  $\mu$ M). Together with our previous study, these data suggest that the  $[DA_p]$  and dopamine peak height are not completely reflective of release, and interpretation is heavily influenced by reduced uptake, where peak height increases but upward velocity does not. In experiments where PTT and WF23 were applied, peak dopamine release was increased over baseline values across concentrations, but with reduced upward velocity in the 3–30  $\mu$ M range. This concentration range coincided with larger reductions in downward velocity. This suggests that the decrease in upward velocity, but overall increase in peak, is due to increased detection of release from

diffusion from distant compartments. In contrast to DAT blocker experiments, there were similar upward velocities observed between WT and DATKO mice. This finding was surprising because DATKO mice have been heavily used as a comparison group for studying clearance kinetics in the absence of the DAT (i.e., diffusion)<sup>34,35</sup> and suggests that there are compensations in DATKO mice affecting release and potentially clearance. Therefore, experiments examining dopamine diffusion may benefit more from using these or other high affinity DAT blockers. These results also support an unknown adaptation in dopamine clearance—possibly secondary clearance mediated by the cholesterol sensitive organic cation transporter.<sup>36</sup>

The diversity of observed effects of DAT inhibitors on peak height and velocity measures of release across concentrations are indicative of the multiple effects of DAT inhibitors on dopamine terminals. One of the mechanisms recruited during DAT blockade is activation of dopamine D<sub>2</sub> type receptors.<sup>37</sup> Dopamine D<sub>2</sub> type receptors are inhibitory GPCRs, located on presynaptic dopamine terminals (as autoreceptors) and on postsynaptic neurons (as heteroreceptors) in the striatum. At the soma, D<sub>2</sub> autoreceptors activate inhibitory effectors, including the G-protein-coupled inward rectifying potassium (GIRK) channels, to drive membrane hyperpolarization.<sup>38</sup> In vivo, cocaine increases dopamine levels,<sup>39</sup> resulting in D<sub>2</sub> mediated inhibition of somatic activity.<sup>40</sup> In a slice, evoked dopamine release is insensitive to D<sub>2</sub> antagonists,<sup>41,42</sup> demonstrating that extracellular tone is minimal in slice conditions. Fast-scan controlled adsorption voltammetry (FSCAV) studies in slices have reported extracellular dopamine levels of ~11 nM in the striatum<sup>43</sup> and ~40 nM in the SNc.<sup>44</sup> Bath application of cocaine (10  $\mu$ M) increased extracellular dopamine in the SNc by ~6.8 nM.<sup>44</sup> There are currently no FSCAV reports on dopamine levels after cocaine in striatal slices. However, bath application of dopamine (1  $\mu$ M) produces modest (~5–10%) activation of D<sub>2</sub> receptors (IC<sub>50</sub> of 36  $\mu$ M), and cocaine (10  $\mu$ M) quadruples D<sub>2</sub> sensitivity (IC<sub>50</sub> at 9  $\mu$ M).<sup>45</sup> Several studies have shown D<sub>2</sub> mediated inhibition of dopamine release with cocaine at high concentrations (10  $\mu$ M).<sup>46,47</sup> We have observed D<sub>2</sub> mediated inhibition of dopamine release by cocaine at concentrations as low as 1  $\mu$ M.<sup>48</sup> At low concentrations insufficient for inhibiting uptake (10 nM), cocaine has been shown to enhance D<sub>2</sub> receptor stimulation possibly due to positive allosteric effects on D<sub>2</sub> receptors.<sup>49–51</sup> Blocking D<sub>2</sub> receptors in the presence of cocaine (1–10  $\mu$ M) results in greater dopamine release.<sup>46–48</sup> Since reductions in dopamine release velocity were observed herein in the presence of the D<sub>2</sub> agonist quinpirole, and since DAT blockers examined are known to increase D<sub>2</sub> activation, the decrease in release velocity observed with DAT blockers can be attributed in part to D<sub>2</sub> autoreceptor activation. In terminals, D<sub>2</sub> activation will likely influence several effectors to attenuate dopamine release, including activation of Kv2.1 channels,<sup>52</sup> inhibition of snare proteins,<sup>53</sup> and inhibition of synthesis proteins (i.e., tyrosine hydroxylase).<sup>54</sup> It is unknown if GABA<sub>B</sub> receptors recruit this same machinery at dopamine terminals, or if some of cocaine's effects are through enhancement of GABA<sub>B</sub> effects. It seems likely that adaptations from cocaine would affect GABA<sub>B</sub> sensitivity considering the overlap in effector coupling for these receptors.<sup>55</sup> Cholinergic interneurons (CINs) are a major regulator of dopamine activity, and electrically evoked dopamine release is initiated in part through release of acetylcholine and subsequent

depolarization through activation of nicotinic acetylcholine receptors (nAChRs).<sup>48,56</sup> Furthermore, nAChR allosteric activators and nAChR blockers enhance and reduce dopamine release, respectively.<sup>48,57</sup> Also, the dopamine release process is dependent on sodium channel mediated depolarization on dopamine terminals,<sup>48</sup> subsequent opening of voltage gated calcium channels,<sup>58</sup> and calcium entry, which interact with snare proteins to trigger vesicular fusion.<sup>59</sup> Cocaine has been shown to block nAChR conductance at concentrations  $>3 \mu\text{M}$ .<sup>60</sup> Mice lacking the  $\beta$ -2 nAChR subunit have reduced sensitivity to inhibition from cocaine.<sup>60</sup> In this latter study, peak reductions still occurred in  $\beta$ -2 knockout mice, but with a considerable reduction in sensitivity. Indeed, attenuated increases were observed in WT mice at concentrations  $>2 \mu\text{M}$  concentrations, but in  $\beta$ -2 knockouts only at concentrations  $>10 \mu\text{M}$ .<sup>60</sup> The inhibition observed at higher concentrations in  $\beta$ -2 knockout mice was attributed to cocaine's well-known anesthetic effect.<sup>60</sup> Since WF23 and PTT share some structural homology with cocaine, it is likely that these drugs are acting through these several mechanisms to attenuate release. However, whether WF23 and PTT have nAChR or anesthetic effects at the tested concentrations remains unknown.

The downward velocity measure was highly indicative of DAT function. Downward velocity significantly correlated with Michaelis–Menten  $V_{\text{max}}$  values in vivo and in slice in WT mice and was considerably reduced in DATKO mice. Furthermore, downward velocity decreased after application of DAT blockers in slice and in vivo. Thus, downward velocity reliably predicts slower DAT kinetics in the presence of blockers. Since DATKO mice have no enzymatic function, the Michaelis–Menten  $V_{\text{max}}$  cannot be used in DATKO analysis. This highlights an important utility of downward velocity in studying dopamine clearance without violating specific enzymatic conditions.

Although data in the present study indicate a clearance mechanism mainly mediated through the DAT, other mechanisms are also involved in clearance. Data from DATKO mice and pharmacological DAT blockade experiments presented herein indicate multiple aspects of dopamine transmission (release and clearance) that are altered under these conditions. Both velocity down and tau measures are slowed in these conditions. Interestingly, with increased stimulation intensity, dopamine clearance rate in DATKO slices was increased, suggesting additional recruited mechanisms of clearance. The organic cation transporter 3 (OCT3) has been implicated in catecholamine clearance in the striatum<sup>61</sup> and basolateral amygdala.<sup>62</sup> DATKO mice have previously been used as a model of diffusion, but recent evidence demonstrates that OCT3 is active and even upregulated in DATKO transgenic rats.<sup>63</sup> While not tested exclusively herein, it is possible that increased stimulation intensity is recruiting this alternate uptake mechanism. Peak height was consistently increased with DAT blockade at low concentrations. This increase in peak height has been observed many times previously, and is attributed to either facilitated release<sup>64</sup> or increased rate of diffusion, resulting in bigger peaks.<sup>22,65</sup> With peak height increasing, we largely saw increased upward velocity with low concentrations of DAT inhibitors, and most robustly with WF-23. The ratio between upward velocity and peak height starts to decrease with higher concentrations, which may be more indicative of increased rate of diffusion due to fewer active DAT sites. Others have

reported increased peak height with slower time to peak in the presence of DAT inhibitors, which is attributed and supportive of this measure as one of increased diffusion.<sup>22,65,66</sup> Importantly, dextran, which is known to slow diffusion rate, also results in increases in peak height in areas where diffusion is a major clearing mechanism.<sup>65</sup>

Other factors can also affect diffusion. The tortuosity of the slice, determined by synaptic and extrasynaptic organization, is a major factor in diffusion and has been shown to be altered in disease states.<sup>67</sup> Whether diffusion is altered in DATKO animals is unknown. Interestingly, we observed similar peak heights between WT and DATKO animals, suggesting similar release. This is surprising since previous studies have observed reduced release in DATKO mice.<sup>68,69</sup> Other recent research has shown increased release in DATKO compared to WT rats,<sup>63</sup> and others have shown no difference.<sup>70</sup> There were no obvious differences in methods to account for these discrepancies. Indeed, the original studies are missing important information (e.g., stimulation intensity, ACSF composition, animal age, etc.) that may contribute to release differences. In speculation, it seems possible that removing the primary mechanism of dopamine clearance from an animal would result in age-specific developmental alterations that are observed in some studies but not others.

Dopamine signaling is observed in other brain areas, and the primary clearance mechanism is not always the DAT (in contrast to striatum), allowing for more volume transmission effects due to diffusion. For example, in olfactory glomeruli, clearance is objectively slower than in striatum and appears to be mediated primarily via the catechol-*O*-methyltransferase (COMT).<sup>71,72</sup> Midbrain and central amygdala signals are also relatively slower than striatum, making diffusion a more important mechanism of clearance in these brain regions.<sup>22,73</sup> Importantly, diffusional impact appears to increase with higher dopamine concentrations, as can be seen in pressure ejection<sup>74</sup> and iontophoresis studies.<sup>75</sup> These studies highlight that various mechanisms play a role in clearance. A 2-compartment diffusion model has been used previously and is a highly effective approach for measuring clearance from exogenous catecholamine perfusion.<sup>67,76,77</sup> It will be interesting to see how the present unbiased measures contribute to these diffusion-based models in the future, as well as how these measures are applied to other neurotransmitters or detection techniques.

In addition to downward velocity, exponential decay (tau) was applied to the data. Increasing concentrations of DAT blockers resulted in higher values of tau ex vivo. These higher values of tau corresponded with the relative potency of the DAT blocker (highest for WF23 and lowest for cocaine). Similarly, in vivo experiments revealed a large increase in tau for mice with WF23 injections and a much smaller increase for mice with PTT injections. This corresponds to the Michaelis–Menten  $K_m$ , which increases with lower enzymatic affinity for a substrate.<sup>5</sup> Thus, the present study asserts the use of both downward velocity and tau as complementary ways to analyze DAT kinetics, independent of the Michaelis–Menten model. We anticipate that the use of the unbiased measures of velocity and exponential decay will be favored by others for their ease of use and reduced user input. We expect that the use of these measures as a complement to Michaelis–Menten approaches may help reduce experimenter error. Lastly, the use of this approach allows for interpretations outside of Michaelis–Menten-based assumptions, for instance in brain regions where



the DAT is not the predominate mode of clearance. This last application will facilitate our understanding of neurotransmitter dynamics and how they are affected in drug and disease states.

## MATERIALS AND METHODS

**Animals.** Male and Female (Jackson Laboratory, Sacramento, CA) WT and DATKO (~25–35 g) mice on C57Bl/6 background were given ad libitum access to food and water and maintained on a 12:12-h light/dark cycle. All protocols and animal care procedures were in accordance with the National Institutes of Health Guide for the Care and Use of Laboratory Animals and approved by Brigham Young University Institutional Animal Care and Use Committee, Oregon Health and Science, Drexel University College of Medicine, and Wake Forest University Health Sciences.

**Brain Slice Preparation and Drug Application.** Isoflurane (Patterson Veterinary, Devens, MA) anesthetized mice were sacrificed by decapitation and brains were rapidly removed, sectioned into thick coronal striatal slices (300–400  $\mu\text{m}$ ; Leica VT1000S, Vashaw Scientific, Norcross, GA), incubated for 60 min at 34 °C in pre-oxygenated (95%  $\text{O}_2$ /5%  $\text{CO}_2$ ) artificial cerebral spinal fluid (aCSF). The aCSF consisted of (in mM): NaCl (126), KCl (2.5),  $\text{NaH}_2\text{PO}_4$  (1.2),  $\text{MgCl}_2$  (1.2),  $\text{NaHCO}_3$  (25), D-glucose (11), L-ascorbic acid (0.4), with pH adjusted to ~7.4. Cutting solution also contained either MK801 (10  $\mu\text{M}$ ; (5S,10R)-(+)-5-methyl-10,11-dihydro-5H-dibenzo[*a,d*]cyclohepten-5,10-imine; Abcam, Cambridge, UK) or kynurenic acid (2 mM) for blockade of ionotropic glutamate receptors. At the end of the incubation period, tissue was transferred to aCSF (34 °C) without glutamate receptor blockers. The following concentrations of drugs were bath applied for slice voltammetry experiments where specified: Baclofen (30  $\mu\text{M}$ ), CGP55845 (200 nM), quinpirole (10  $\mu\text{M}$ ), sulpiride (600 nM; Sigma), 2 $\beta$ -propanoyl-3 $\beta$ -(2-naphthyl)-tropane (WF-23) (10 nM–3  $\mu\text{M}$ ; Huw M. L. Davies, Emory University, Atlanta, GA), 2 $\beta$ -propanoyl-3 $\beta$ -(4-tolyl)-tropane (PTT) (100 nM–30  $\mu\text{M}$ ; Huw M. L. Davies), cocaine (300 nM–30  $\mu\text{M}$ ; NIDA, Rockville, MD, USA).

**Ex Vivo Voltammetry Recordings.** Slices were transferred to the recording chamber, and perfused with aCSF (34 °C) at a rate of ~1.8 mL/min. FSCV recordings were performed and analyzed using Demon Voltammetry and Analysis software.<sup>6</sup> Carbon fiber electrodes used in voltammetry experiments were made in-house. The carbon fiber (7  $\mu\text{m}$  diameter, Thornel T-650, Cytec, Woodland Park, NJ) was aspirated into a borosilicate glass capillary tube (TW150, World Precision Instruments, Sarasota, FL). Electrodes were then pulled using a pipette puller and cut so that 100–150  $\mu\text{m}$  of carbon fiber protruded from the tip of the glass. The electrode potential was linearly scanned as a triangular waveform from –0.4 to 1.2 V and back to –0.4 V (Ag vs AgCl) with a scan rate of 400 V/s, repeated every 100 ms. Carbon fiber electrodes were positioned ~250  $\mu\text{m}$  below the slice surface. For baclofen and quinpirole experiments, dopamine release was evoked through electrical stimulation (1 pulse/min) via a glass micropipette (30  $\mu\text{A}$ , 0.5 ms), repeated every 2 min. For calcium and DATKO experiments, dopamine release was evoked from a bipolar stimulating electrode (Plastics One, Roanoke, VA) with stimulations at 1 pulse, 5 pulses at 20 Hz, or 24 pulses at 60 Hz (300  $\mu\text{A}$ , 4 msec) applied to the tissue every 5 min. Multiple pulse stimulation parameters were selected to model the different in vivo firing patterns of dopamine neurons.<sup>78,79</sup> For baseline collections, stimulations were applied every 2 or 5 min until a stable baseline was established (3 collections within 10% variability). Next, either drug or stimulation conditions were changed as noted in the results.

**In Vivo Voltammetry Recordings.** On the day of testing, mice were anesthetized with urethane (1.5 g/kg, i.p.; Sigma-Aldrich, St. Louis, MO, USA) and implanted with an intravenous (i.v.) catheter as previously described.<sup>80,81</sup> All drugs for in vivo experiments were dissolved in 0.9% saline. Mice were subsequently placed in a stereotaxic apparatus while a stimulating electrode was lowered into the ventral tegmental area (VTA) (–3.0 A/P, +1.0 M/L, –4.5–5.0 D/V), a carbon fiber electrode was lowered into the dorsal caudate

(+1.3 A/P, +1.3 M/L, –3.0 D/V) and a reference electrode was implanted in the contralateral cortex (+1.5 A/P, –1.5 M/L, –2.0 D/V).<sup>81</sup> Dopamine release was elicited via electrical stimulation of the VTA using 0.4–1 s, 60 Hz monophasic (24p, 4 ms; ~400  $\mu\text{A}$ ) stimulation trains. The length of stimulation was varied to ensure sufficient dopamine release across experiments. Baseline dopamine response parameters were collected in 5-min intervals for a minimum of 30 min prior to drug injection. Once a stable baseline of three consecutive collections was obtained (defined as dopamine peak height within 15%), mice received a single ~200  $\mu\text{L}$  i.v. (2 s) injection of WF-23 (5.0 mg/kg  $n$  = 7), PTT (5.0 mg/kg  $n$  = 7) or cocaine (1.5 mg/kg  $n$  = 6). Evoked dopamine release was measured at 30- and 60-s post injection and every 5 min thereafter until a peak drug effect was established.

**Data Analysis and Statistics.** The magnitude of electrically evoked dopamine release (peak height) and transporter-mediated uptake were monitored and dopamine overflow curves were fitted to an exponential decay model and expressed as tau (time to ~33% of peak height; units in seconds). Data were also modeled using the Michaelis–Menten fit or using the fastest upward or downward velocity calculated from the first derivative of the release trace. All data were analyzed using Demon Voltammetry and Analysis software<sup>6</sup> written in LabVIEW (National Instruments, Austin, TX).

Carbon fiber electrodes were initially calibrated using low (1  $\mu\text{M}$ ) and high (10  $\mu\text{M}$ ) dopamine concentrations, which was compared back to background current amplitude for establishing a model based on linear regression for calibration values. The resultant linear regression model was applied to electrodes for determining the relative calibration constant. Statistics were performed using Prism 5 (GraphPad, San Diego, CA) and NCSS 8 (NCSS LLC, Kaysville, UT). Statistical significance was determined for groups of two variables using a two-tailed Student's *t*-test. Experiments with more than two groups, but only one factor, were tested for significance using a one-way analysis of variance (ANOVA). Data from multiple time points within the same experiment were analyzed with a repeated measures ANOVA (RM-ANOVA). For experiments that examined multiple factors and interactions, two-way ANOVA or RM-ANOVAs were used. Tukey's HSD and Bonferroni correction methods were used for post-ANOVA analysis. For figures where raw traces are shown that are described as having “slow” or “fast” downward velocity (e.g., Figures 4 and 7), no specific threshold was used for labeling a signal as “slow” or “fast”; described velocity is relative to other experiments from the same dataset.

## ASSOCIATED CONTENT

### Supporting Information

The Supporting Information is available free of charge at <https://pubs.acs.org/doi/10.1021/acscchemneuro.2c00033>.

Comparison between upward velocity and Michaelis–Menten  $V_{\text{max}}$ . Comparison between downward velocity and exponential decay (tau). Both comparisons are made with slice and in vivo data (PDF)

## AUTHOR INFORMATION

### Corresponding Author

Jordan T. Yorgason – Department of Cellular Biology and Physiology, Brigham Young University, Provo, Utah 84602, United States; [orcid.org/0000-0002-5687-0676](https://orcid.org/0000-0002-5687-0676); Email: [jordanyorg@byu.edu](mailto:jordanyorg@byu.edu)

### Authors

Anna C. Everett – Department of Cellular Biology and Physiology, Brigham Young University, Provo, Utah 84602, United States

Ben E. Graul – Department of Cellular Biology and Physiology, Brigham Young University, Provo, Utah 84602, United States



Joakim W. Ronström – Department of Cellular Biology and Physiology, Brigham Young University, Provo, Utah 84602, United States

J. Kayden Robinson – Department of Cellular Biology and Physiology, Brigham Young University, Provo, Utah 84602, United States

Daniel B. Watts – Department of Cellular Biology and Physiology, Brigham Young University, Provo, Utah 84602, United States

Rodrigo A. España – Department of Neurobiology & Anatomy, Drexel University, Philadelphia, Pennsylvania 19122, United States

Cody A. Siciliano – Center for Addiction Research, Vanderbilt University, Nashville, Tennessee 37203, United States

Complete contact information is available at:

<https://pubs.acs.org/10.1021/acschemneuro.2c00033>

### Author Contributions

A.C.E., R.A.E., C.A.S. and J.T.Y. designed experiments and performed the research. A.C.E., B.E.G., D.B.W., J.K.R. and J.T.Y. analyzed and interpreted experiments. J.T.Y. wrote additional software for analysis. A.C.E., B.E.G., J.W.R. and J.T.Y. contributed to manuscript writing.

### Notes

The authors declare no competing financial interest.

### ACKNOWLEDGMENTS

This work is supported by the US National Institute of Health (NIH) grants DA040409 to J.T.Y., R00 DA04510 to C.A.S., R01031900 to R.A.E. as well as grants from the Brain and Behavior Research Foundation and Alkermes to C.A.S., and internal mentored research funding from Brigham Young University College of Life Sciences to J.T.Y. We would also like to thank Caylor Hafen, Hillary Wadsworth, Parker Layton for their help in performing blinded Michaelis–Menten analysis. We would also like to thank Jared Willets for assistance in graphic design.

### REFERENCES

- (1) Ferris, M. J.; Calipari, E. S.; Yorgason, J. T.; Jones, S. R. Examining the complex regulation and drug-induced plasticity of dopamine release and uptake using voltammetry in brain slices. *ACS Chem. Neurosci.* **2013**, *4*, 693–703.
- (2) Li, Y.; Ross, A. E. Plasma-treated carbon-fiber microelectrodes for improved purine detection with fast-scan cyclic voltammetry. *Analyst* **2020**, *145*, 805–815.
- (3) Spanos, M.; Gras-Najjar, J.; Letchworth, J. M.; Sanford, A. L.; Toups, J. V.; Sombers, L. A. Quantitation of hydrogen peroxide fluctuations and their modulation of dopamine dynamics in the rat dorsal striatum using fast-scan cyclic voltammetry. *ACS Chem. Neurosci.* **2013**, *4*, 782–789.
- (4) Wightman, R. M. Voltammetry with microscopic electrodes in new domains. *Science* **1988**, *240*, 415–420.
- (5) Wightman, R. M.; Zimmerman, J. B. Control of dopamine extracellular concentration in rat striatum by impulse flow and uptake. *Brain Res. Brain Res. Rev.* **1990**, *15*, 135–144.
- (6) Yorgason, J. T.; España, R. A.; Jones, S. R. Demon voltammetry and analysis software: analysis of cocaine-induced alterations in dopamine signaling using multiple kinetic measures. *J. Neurosci. Methods* **2011**, *202*, 158–164.
- (7) Wu, Q.; Reith, M. E. A.; Kuhar, M. J.; Carroll, F. I.; Garriss, P. A. Preferential increases in nucleus accumbens dopamine after systemic cocaine administration are caused by unique characteristics of dopamine neurotransmission. *J. Neurosci.* **2001**, *21*, 6338–6347.
- (8) Michaelis, L.; Menten, M. L.; Johnson, K. A.; Goody, R. S. The original Michaelis constant: translation of the 1913 Michaelis-Menten paper. *Biochemistry* **2011**, *50*, 8264–8269.
- (9) Lopachev, A.; Volnova, A.; Evdokimenko, A.; Abaimov, D.; Timoshina, Y.; Kazanskaya, R.; Lopacheva, O.; Deal, A.; Budygin, E.; Fedorova, T.; Gainetdinov, R. Intracerebroventricular injection of ouabain causes mania-like behavior in mice through D2 receptor activation. *Sci. Rep.* **2019**, *9*, 15627.
- (10) Pattison, L. P.; McIntosh, S.; Budygin, E. A.; Hemby, S. E. Differential regulation of accumbal dopamine transmission in rats following cocaine, heroin and speedball self-administration. *J. Neurochem.* **2012**, *122*, 138–146.
- (11) John, C. E.; Jones, S. R. Voltammetric characterization of the effect of monoamine uptake inhibitors and releasers on dopamine and serotonin uptake in mouse caudate-putamen and substantia nigra slices. *Neuropharmacology* **2007**, *52*, 1596–1605.
- (12) Xiao, N.; Privman, E.; Venton, B. J. Optogenetic control of serotonin and dopamine release in *Drosophila* larvae. *ACS Chem. Neurosci.* **2014**, *5*, 666–673.
- (13) Near, J. A.; Bigelow, J. C.; Wightman, R. M. Comparison of uptake of dopamine in rat striatal chopped tissue and synaptosomes. *J. Pharmacol. Exp. Ther.* **1988**, *245*, 921–927.
- (14) Torres, D. J.; Yorgason, J. T.; Andres, M. A.; Bellinger, F. P. *Methamphetamine Exposure During Development Causes Lasting Changes to Mesolimbic Dopamine Signaling in Mice*. *Cell Mol. Neurobiol.* **2021**, DOI: 10.1007/s10571-021-01120-4.
- (15) Yorgason, J. T.; España, R. A.; Konstantopoulos, J. K.; Weiner, J. L.; Jones, S. R. Enduring increases in anxiety-like behavior and rapid nucleus accumbens dopamine signaling in socially isolated rats. *Eur. J. Neurosci.* **2013**, *37*, 1022–1031.
- (16) Calipari, E. S.; Ferris, M. J.; Siciliano, C. A.; Jones, S. R. Differential influence of dopamine transport rate on the potencies of cocaine, amphetamine, and methylphenidate. *ACS Chem. Neurosci.* **2015**, *6*, 155–162.
- (17) Ramsson, E. S.; Covey, D. P.; Daberkow, D. P.; Litherland, M. T.; Juliano, S. A.; Garriss, P. A. Amphetamine augments action potential-dependent dopaminergic signaling in the striatum in vivo. *J. Neurochem.* **2011**, *117*, 937–948.
- (18) Siciliano, C. A.; Mauterer, M. I.; Fordahl, S. C.; Jones, S. R. Modulation of striatal dopamine dynamics by cocaine self-administration and amphetamine treatment in female rats. *Eur. J. Neurosci.* **2019**, *50*, 2740–2749.
- (19) Yorgason, J. T.; Calipari, E. S.; Ferris, M. J.; Karkhanis, A. N.; Fordahl, S. C.; Weiner, J. L.; Jones, S. R. Social isolation rearing increases dopamine uptake and psychostimulant potency in the striatum. *Neuropharmacology* **2016**, *101*, 471–479.
- (20) Torres, D. J.; Yorgason, J. T.; Mitchell, C. C.; Hagiwara, A.; Andres, M. A.; Kurokawa, S.; Steffensen, S. C.; Bellinger, F. P. Selenoprotein P Modulates Methamphetamine Enhancement of Vesicular Dopamine Release in Mouse Nucleus Accumbens Via Dopamine D2 Receptors. *Front. Neurosci.* **2021**, *15*, No. 631825.
- (21) Yorgason, J. T.; Ferris, M. J.; Steffensen, S. C.; Jones, S. R. Frequency-dependent effects of ethanol on dopamine release in the nucleus accumbens. *Alcohol Clin. Exp. Res.* **2014**, *38*, 438–447.
- (22) Ford, C. P.; Gantz, S. C.; Phillips, P. E. M.; Williams, J. T. Control of extracellular dopamine at dendrite and axon terminals. *J. Neurosci.* **2010**, *30*, 6975–6983.
- (23) Karkhanis, A. N.; Leach, A. C.; Yorgason, J. T.; Uneri, A.; Barth, S.; Niere, F.; Alexander, N. J.; Weiner, J. L.; McCool, B. A.; Raab-Graham, K. F.; Ferris, M. J.; Jones, S. R. Chronic Social Isolation Stress during Peri-Adolescence Alters Presynaptic Dopamine Terminal Dynamics via Augmentation in Accumbal Dopamine Availability. *ACS Chem. Neurosci.* **2019**, *10*, 2033–2044.
- (24) Bisgaard, H.; Larsen, M. A.; Mazier, S.; Beuming, T.; Newman, A. H.; Weinstein, H.; Shi, L.; Loland, C. J.; Gether, U. The binding sites for benzotropines and dopamine in the dopamine transporter overlap. *Neuropharmacology* **2011**, *60*, 182–190.
- (25) Beuming, T.; Kniazeff, J.; Bergmann, M. L.; Shi, L.; Gracia, L.; Raniszewska, K.; Newman, A. H.; Javitch, J. A.; Weinstein, H.; Gether,

- U.; Loland, C. J. The binding sites for cocaine and dopamine in the dopamine transporter overlap. *Nat. Neurosci.* **2008**, *11*, 780–789.
- (26) Wang, K. H.; Penmatsa, A.; Gouaux, E. Neurotransmitter and psychostimulant recognition by the dopamine transporter. *Nature* **2015**, *521*, 322–327.
- (27) Davies, H. M. L.; Saikali, E.; Huby, N. J. S.; Gilliatt, V. J.; Matasi, J. J.; Sexton, T.; Childers, S. R. Synthesis of 2 beta-acyl-3 beta-aryl-8-azabicyclo[3.2.1]octanes and their binding affinities at dopamine and serotonin transport sites in rat striatum and frontal cortex. *J. Med. Chem.* **1994**, *37*, 1262–1268.
- (28) Bennett, B. A.; Wichems, C. H.; Hollingsworth, C. K.; Davies, H. M.; Thornley, C.; Sexton, T.; Childers, S. R. Novel 2-substituted cocaine analogs: uptake and ligand binding studies at dopamine, serotonin and norepinephrine transport sites in the rat brain. *J. Pharmacol. Exp. Ther.* **1995**, *272*, 1176–1186.
- (29) Letchworth, S. R.; Smith, H. R.; Porrino, L. J.; Bennett, B. A.; Davies, H. M.; Sexton, T.; Childers, S. R. Characterization of a tropane radioligand, [(3H)]2beta-propanoyl-3beta-(4-tolyl) tropane ([[(3H)]PTT]), for dopamine transport sites in rat brain. *J. Pharmacol. Exp. Ther.* **2000**, *293*, 686–696.
- (30) Gatley, S. J.; Pan, D.; Chen, R.; Chaturvedi, G.; Ding, Y. S. Affinities of methylphenidate derivatives for dopamine, norepinephrine and serotonin transporters. *Life Sci.* **1996**, *58*, 231–239.
- (31) Katz, J. L.; Izenwasser, S.; Terry, P. Relationships among dopamine transporter affinities and cocaine-like discriminative-stimulus effects. *Psychopharmacology* **2000**, *148*, 90–98.
- (32) Calipari, E. S.; Ferris, M. J.; Siciliano, C. A.; Zimmer, B. A.; Jones, S. R. Intermittent cocaine self-administration produces sensitization of stimulant effects at the dopamine transporter. *J. Pharmacol. Exp. Ther.* **2014**, *349*, 192–198.
- (33) Siciliano, C. A.; Calipari, E. S.; Ferris, M. J.; Jones, S. R. Adaptations of presynaptic dopamine terminals induced by psychostimulant self-administration. *ACS Chem. Neurosci.* **2015**, *6*, 27–36.
- (34) Jones, S. R.; Gainetdinov, R. R.; Wightman, R. M.; Caron, M. G. Mechanisms of amphetamine action revealed in mice lacking the dopamine transporter. *J. Neurosci.* **1998**, *18*, 1979–1986.
- (35) Benoit-Marand, M.; Jaber, M.; Gonon, F. Release and elimination of dopamine in vivo in mice lacking the dopamine transporter: functional consequences. *Eur. J. Neurosci.* **2000**, *12*, 2985–2992.
- (36) Gasser, P. J. Roles for the uptake2 transporter OCT3 in regulation of dopaminergic neurotransmission and behavior. *Neurochem. Int.* **2019**, *123*, 46–49.
- (37) Kimmel, H. L.; Joyce, A. R.; Carroll, F. I.; Kuhar, M. J. Dopamine D1 and D2 receptors influence dopamine transporter synthesis and degradation in the rat. *J. Pharmacol. Exp. Ther.* **2001**, *298*, 129–140.
- (38) Pillai, G.; Brown, N. A.; McAllister, G.; Milligan, G.; Seabrook, G. R. Human D2 and D4 dopamine receptors couple through betagamma G-protein subunits to inwardly rectifying K<sup>+</sup> channels (GIRK1) in a *Xenopus* oocyte expression system: selective antagonism by L-741,626 and L-745,870 respectively. *Neuropharmacology* **1998**, *37*, 983–987.
- (39) Greco, P. G.; Garriss, P. A. In vivo interaction of cocaine with the dopamine transporter as measured by voltammetry. *Eur. J. Pharmacol.* **2003**, *479*, 117–125.
- (40) Einhorn, L. C.; Johansen, P. A.; White, F. J. Electrophysiological effects of cocaine in the mesoaccumbens dopamine system: studies in the ventral tegmental area. *J. Neurosci.* **1988**, *8*, 100–112.
- (41) Phillips, P. E. M.; Hancock, P. J.; Stamford, J. A. Time window of autoreceptor-mediated inhibition of limbic and striatal dopamine release. *Synapse* **2002**, *44*, 15–22.
- (42) Kennedy, R. T.; Jones, S. R.; Wightman, R. M. Dynamic observation of dopamine autoreceptor effects in rat striatal slices. *J. Neurochem.* **1992**, *59*, 449–455.
- (43) Burrell, M. H.; Atcherley, C. W.; Heien, M. L.; Lipski, J. A novel electrochemical approach for prolonged measurement of absolute levels of extracellular dopamine in brain slices. *ACS Chem. Neurosci.* **2015**, *6*, 1802–1812.
- (44) Yee, A. G.; Forbes, B.; Cheung, P. Y.; Martini, A.; Burrell, M. H.; Freestone, P. S.; Lipski, J. Action potential and calcium dependence of tonic somatodendritic dopamine release in the Substantia Nigra pars compacta. *J. Neurochem.* **2019**, *148*, 462–479.
- (45) Marcott, P. F.; Mamaligas, A. A.; Ford, C. P. Phasic dopamine release drives rapid activation of striatal D2-receptors. *Neuron* **2014**, *84*, 164–176.
- (46) Holroyd, K. B.; Adrover, M. F.; Fuino, R. L.; Bock, R.; Kaplan, A. R.; Gremel, C. M.; Rubinstein, M.; Alvarez, V. A. Loss of feedback inhibition via D2 autoreceptors enhances acquisition of cocaine taking and reactivity to drug-paired cues. *Neuropsychopharmacology* **2015**, *40*, 1495–1509.
- (47) Adrover, M. F.; Shin, J. H.; Alvarez, V. A. Glutamate and dopamine transmission from midbrain dopamine neurons share similar release properties but are differentially affected by cocaine. *J. Neurosci.* **2014**, *34*, 3183–3192.
- (48) Yorgason, J. T.; Zeppenfeld, D. M.; Williams, J. T. Cholinergic Interneurons Underlie Spontaneous Dopamine Release in Nucleus Accumbens. *J. Neurosci.* **2017**, *37*, 2086–2096.
- (49) Ferraro, L.; Beggiato, S.; Marcellino, D.; Frankowska, M.; Filip, M.; Agnati, L. F.; Antonelli, T.; Tomasini, M. C.; Tanganelli, S.; Fuxe, K. Nanomolar concentrations of cocaine enhance D2-like agonist-induced inhibition of the K<sup>+</sup>-evoked [3H]-dopamine efflux from rat striatal synaptosomes: a novel action of cocaine. *J. Neural. Transm. (Vienna)* **2010**, *117*, 593–597.
- (50) Genedani, S.; Carone, C.; Guidolin, D.; Filaferro, M.; Marcellino, D.; Fuxe, K.; Agnati, L. F. Differential sensitivity of A2A and especially D2 receptor trafficking to cocaine compared with lipid rafts in cotransfected CHO cell lines. Novel actions of cocaine independent of the DA transporter. *J. Mol. Neurosci.* **2010**, *41*, 347–357.
- (51) Ferraro, L.; Frankowska, M.; Marcellino, D.; Zaniewska, M.; Beggiato, S.; Filip, M.; Tomasini, M. C.; Antonelli, T.; Tanganelli, S.; Fuxe, K. A novel mechanism of cocaine to enhance dopamine d2-like receptor mediated neurochemical and behavioral effects. An in vivo and in vitro study. *Neuropsychopharmacology* **2012**, *37*, 1856–1866.
- (52) Fulton, S.; Thibault, D.; Mendez, J. A.; Lahaie, N.; Tirotta, E.; Borrelli, E.; Bouvier, M.; Tempel, B. L.; Trudeau, L. E. Contribution of Kv1.2 voltage-gated potassium channel to D2 autoreceptor regulation of axonal dopamine overflow. *J. Biol. Chem.* **2011**, *286*, 9360–9372.
- (53) Blackmer, T.; Larsen, E. C.; Takahashi, M.; Martin, T. F. J.; Alford, S.; Hamm, H. E. G protein betagamma subunit-mediated presynaptic inhibition: regulation of exocytotic fusion downstream of Ca<sup>2+</sup> entry. *Science* **2001**, *292*, 293–297.
- (54) Chen, R.; Ferris, M. J.; Wang, S. Dopamine D2 autoreceptor interactome: Targeting the receptor complex as a strategy for treatment of substance use disorder. *Pharmacol. Ther.* **2020**, *213*, No. 107583.
- (55) Guatteo, E.; Bengtson, C. P.; Bernardi, G.; Mercuri, N. B. Voltage-gated calcium channels mediate intracellular calcium increase in weaver dopaminergic neurons during stimulation of D2 and GABAB receptors. *J. Neurophysiol.* **2004**, *92*, 3368–3374.
- (56) Wang, L.; Zhang, X.; Xu, H.; Zhou, L.; Jiao, R.; Liu, W.; Zhu, F.; Kang, X.; Liu, B.; Teng, S.; Wu, Q.; Li, M.; Dou, H.; Zuo, P.; Wang, C.; Wang, S.; Zhou, Z. Temporal components of cholinergic terminal to dopaminergic terminal transmission in dorsal striatum slices of mice. *J. Physiol.* **2014**, *592*, 3559–3576.
- (57) Gao, F.; Chen, D.; Ma, X.; Sudweeks, S.; Yorgason, J. T.; Gao, M.; Turner, D.; Eaton, J. B.; McIntosh, J. M.; Lukas, R. J.; Whiteaker, P.; Chang, Y.; Steffensen, S. C.; Wu, J. Alpha6-containing nicotinic acetylcholine receptor is a highly sensitive target of alcohol. *Neuropharmacology* **2019**, *149*, 45–54.
- (58) Brimblecombe, K. R.; Gracie, C. J.; Platt, N. J.; Cragg, S. J. Gating of dopamine transmission by calcium and axonal N-, Q-, T- and L-type voltage-gated calcium channels differs between striatal domains. *J. Physiol.* **2015**, *593*, 929–946.

- (59) Chen, Y. A.; Scales, S. J.; Patel, S. M.; Doung, Y. C.; Scheller, R. H. SNARE complex formation is triggered by  $\text{Ca}^{2+}$  and drives membrane fusion. *Cell* **1999**, *97*, 165–174.
- (60) Acevedo-Rodriguez, A.; Zhang, L.; Zhou, F.; Gong, S.; Gu, H.; De Biasi, M.; Zhou, F. M.; Dani, J. A. Cocaine inhibition of nicotinic acetylcholine receptors influences dopamine release. *Front. Synaptic Neurosci.* **2014**, *6*, 19.
- (61) Wheeler, D. S.; Ebben, A. L.; Kurtoglu, B.; Lovell, M. E.; Bohn, A. T.; Jasek, I. A.; Baker, D. A.; Mantsch, J. R.; Gasser, P. J.; Wheeler, R. A. Corticosterone regulates both naturally occurring and cocaine-induced dopamine signaling by selectively decreasing dopamine uptake. *Eur. J. Neurosci.* **2017**, *46*, 2638–2646.
- (62) Holleran, K. M.; Rose, J. H.; Fordahl, S. C.; Benton, K. C.; Rohr, K. E.; Gasser, P. J.; Jones, S. R. Organic cation transporter 3 and the dopamine transporter differentially regulate catecholamine uptake in the basolateral amygdala and nucleus accumbens. *Eur. J. Neurosci.* **2020**, *52*, 4546–4562.
- (63) Lloyd, J. T.; Yee, A. G.; Kalligappa, P. K.; Javed, A.; Cheung, P. Y.; Todd, K. L.; Karunasinghe, R. N.; Vlajkovic, S. M.; Freestone, P. S.; Lipski, J. Dopamine Dysregulation and Altered Responses to Drugs Affecting Dopaminergic Transmission in a New Dopamine Transporter Knockout (DAT-KO) Rat Model. *Neuroscience* **2022**, *491*, 43–64.
- (64) Kile, B. M.; Guillot, T. S.; Venton, B. J.; Wetsel, W. C.; Augustine, G. J.; Wightman, R. M. Synapsins differentially control dopamine and serotonin release. *J. Neurosci.* **2010**, *30*, 9762–9770.
- (65) Courtney, N. A.; Ford, C. P. The timing of dopamine- and noradrenaline-mediated transmission reflects underlying differences in the extent of spillover and pooling. *J. Neurosci.* **2014**, *34*, 7645–7656.
- (66) Ford, C. P.; Phillips, P. E. M.; Williams, J. T. The time course of dopamine transmission in the ventral tegmental area. *J. Neurosci.* **2009**, *29*, 13344–13352.
- (67) Syková, E.; Nicholson, C. Diffusion in brain extracellular space. *Physiol. Rev.* **2008**, *88*, 1277–1340.
- (68) Giros, B.; Jaber, M.; Jones, S. R.; Wightman, R. M.; Caron, M. G. Hyperlocomotion and indifference to cocaine and amphetamine in mice lacking the dopamine transporter. *Nature* **1996**, *379*, 606–612.
- (69) Jones, S. R.; Gainetdinov, R. R.; Jaber, M.; Giros, B.; Wightman, R. M.; Caron, M. G. Profound neuronal plasticity in response to inactivation of the dopamine transporter. *Proc. Natl. Acad. Sci. U. S. A.* **1998**, *95*, 4029–4034.
- (70) Leo, D.; Sukhanov, I.; Zoratto, F.; Illiano, P.; Caffino, L.; Sanna, F.; Messa, G.; Emanuele, M.; Esposito, A.; Dorofeikova, M.; Budygin, E. A.; Mus, L.; Efimova, E. V.; Niello, M.; Espinoza, S.; Sotnikova, T. D.; Hoener, M. C.; Laviola, G.; Fumagalli, F.; Adriani, W.; Gainetdinov, R. R. Pronounced Hyperactivity, Cognitive Dysfunctions, and BDNF Dysregulation in Dopamine Transporter Knock-out Rats. *J. Neurosci.* **2018**, *38*, 1959–1972.
- (71) Vaaga, C. E.; Yorgason, J. T.; Williams, J. T.; Westbrook, G. L. Presynaptic gain control by endogenous cotransmission of dopamine and GABA in the olfactory bulb. *J. Neurophysiol.* **2017**, *117*, 1163–1170.
- (72) Cockerham, R.; Liu, S.; Cachope, R.; Kiyokage, E.; Cheer, J. F.; Shipley, M. T.; Puche, A. C. Subsecond Regulation of Synaptically Released Dopamine by COMT in the Olfactory Bulb. *J. Neurosci.* **2016**, *36*, 7779–7785.
- (73) Hedges, D. M.; Yorgason, J. T.; Brundage, J. N.; Wadsworth, H. A.; Williams, B.; Steffensen, S. C.; Roberto, M. Corticotropin releasing factor, but not alcohol, modulates norepinephrine release in the rat central nucleus of the amygdala. *Neuropharmacology* **2020**, *179*, No. 108293.
- (74) Vickrey, T. L.; Xiao, N.; Venton, B. J. Kinetics of the dopamine transporter in *Drosophila* larva. *ACS Chem. Neurosci.* **2013**, *4*, 832–837.
- (75) Nicholson, C. Interaction between diffusion and Michaelis-Menten uptake of dopamine after iontophoresis in striatum. *Biophys. J.* **1995**, *68*, 1699–1715.
- (76) Walters, S. H.; Taylor, I. M.; Shu, Z.; Michael, A. C. A novel restricted diffusion model of evoked dopamine. *ACS Chem. Neurosci.* **2014**, *5*, 776–783.
- (77) Hoffman, A. F.; Spivak, C. E.; Lupica, C. R. Enhanced Dopamine Release by Dopamine Transport Inhibitors Described by a Restricted Diffusion Model and Fast-Scan Cyclic Voltammetry. *ACS Chem. Neurosci.* **2016**, *7*, 700–709.
- (78) Daberkow, D. P.; Brown, H. D.; Bunner, K. D.; Kraniotis, S. A.; Doellman, M. A.; Ragozzino, M. E.; Garriss, P. A.; Roitman, M. F. Amphetamine paradoxically augments exocytotic dopamine release and phasic dopamine signals. *J. Neurosci.* **2013**, *33*, 452–463.
- (79) Zhang, L.; Doyon, W. M.; Clark, J. J.; Phillips, P. E. M.; Dani, J. A. Controls of tonic and phasic dopamine transmission in the dorsal and ventral striatum. *Mol. Pharmacol.* **2009**, *76*, 396–404.
- (80) Yorgason, J. T.; Jones, S. R.; España, R. A. Low and high affinity dopamine transporter inhibitors block dopamine uptake within 5 sec of intravenous injection. *Neuroscience* **2011**, *182*, 125–132.
- (81) Shaw, J. K.; Ferris, M. J.; Locke, J. L.; Brodnik, Z. D.; Jones, S. R.; España, R. A. Hypocretin/orexin knock-out mice display disrupted behavioral and dopamine responses to cocaine. *Addict. Biol.* **2017**, *22*, 1695–1705.

## Recommended by ACS

### Characterization of D3 Autoreceptor Function in Whole Zebrafish Brain with Fast-Scan Cyclic Voltammetry

Piyanka Hettiarachchi and Michael A. Johnson

SEPTEMBER 13, 2022  
ACS CHEMICAL NEUROSCIENCE

READ 

### Neurochemical Concentration Prediction Using Deep Learning vs Principal Component Regression in Fast Scan Cyclic Voltammetry: A Comparison Study

Hoseok Choi, Dong Pyo Jang, *et al.*

JULY 25, 2022  
ACS CHEMICAL NEUROSCIENCE

READ 

### Second-Derivative-Based Background Drift Removal for a Tonic Dopamine Measurement in Fast-Scan Cyclic Voltammetry

Seongtak Kang, Ji-Woong Choi, *et al.*

AUGUST 08, 2022  
ANALYTICAL CHEMISTRY

READ 

### Dopamine Release Impairments Accompany Locomotor and Cognitive Deficiencies in Rotenone-Treated Parkinson's Disease Model Zebrafish

Piyanka Hettiarachchi, Michael A. Johnson, *et al.*

SEPTEMBER 30, 2022  
CHEMICAL RESEARCH IN TOXICOLOGY

READ 

Get More Suggestions >